Myogenesis of Siboglinum Fiordicum Sheds Light on Body Regionalisation in Beard Worms (Siboglinidae, Annelida)

Nadezhda Nikolaevna Rimskaya-Korsakova (rimskaya-korsakova@mail.bio.msu.ru)
Lomonosov Moscow State University https://orcid.org/0000-0001-9576-2435

Nadezda Karaseva
Lomonosov Moscow State University Faculty of Biology: Moskovskij gosudarstvennyj universitet imeni M V Lomonosova Biologiceskij fakul'tet

Timofei Pimenov
Lomonosov Moscow State University Faculty of Biology: Moskovskij gosudarstvennyj universitet imeni M V Lomonosova Biologiceskij fakul'tet

Hans Tore Rapp
University of Bergen: Universitetet i Bergen

Eve Southward
The Marine Biological Association

Elena Temereva
Lomonosov Moscow State University Faculty of Biology: Moskovskij gosudarstvennyj universitet imeni M V Lomonosova Biologiceskij fakul'tet

Katrine Worsaae
University of Copenhagen: Kobenhavns Universitet

Research

Keywords: confocal laser scanning microscopy, 5-actin, transmission electron microscopy, septa, ultrastructure, frenulate pogonophorans, opisthosoma

Posted Date: May 19th, 2021

DOI: https://doi.org/10.21203/rs.3.rs-517176/v1

Abstract

Background

Many annelids, including well-studied species such as *Platynereis*, show similar structured segments along their body axis (homonomous segmentation). However, numerous annelid species diverge from this pattern and exhibit specialised segments or body regions (heteronomous segmentation). Recent phylogenomic studies and paleontological findings suggest that a heteronomous body architecture may represent an ancestral condition in Annelida. To better understand the segmentation within heteronomous species we describe the myogenesis and mesodermal delineation of segments in *Siboglinum fiordicum* during development.

Results

Employing confocal and transmission electron microscopy we show that the somatic circular musculature lies inside the longitudinal musculature and is predominantly developed at the anterior end of the larva. The longitudinal musculature consists of four separate strands at the ventral, dorsal, and ventrolateral body sides. Posteriorly, the longitudinal strands form a continuous layer. Our application of transmission electron microscopy allows us to describe the developmental order of the non-muscular septa. The first septum to form is supported by thick bundles of longitudinal muscles and separates the body into an anterior and a posterior region. The second group of septa to develop further divides the posterior body region (opisthosoma) and is supported by developing circular muscles. At the late larval stage, a septum reinforced by circular muscles divides the anterior body region into a forepart and a trunk segment. The remaining septa and their circular muscles form one by one at the very posterior end of the opisthosoma. Functionally, the prominent ventrolateral longitudinal muscles in the larva are proposed to drive the search movements of the head, while the anterior circular muscles and the posterior continuous layers of longitudinal muscles support the burrowing behaviour of the larva.

Conclusions

The heteronomous *Siboglinum* lacks the strict anterior to posterior sequence of segment formation as it is found in the most studied annelid species. Instead, the first septum divides the body into two body regions, before segments are layed down in first the posterior opisthosoma and then in the anterior body, respectively. Similar pattern of segment formation is described for the heteronomous chaetopterid *Chaetopterus variopedatus* and may represent an ancestral segmentation process in Annelida.

Background

The body plan of annelids is in textbooks often presented as a regular series of segments, similar in structure and function. Such a homonomous (similar) organization is demonstrated in the well-studied Errantian model annelid *Platynereis dumerilii* (1, 2). However, many annelids (as well as arthropods) have heteronomous (irregular) segmentation, where groups of segments are specialized to perform certain

functions, for example, reproduction, mating, feeding, gas exchange, tube construction, etc. (3, 4). Such a "division of labor", manifested in the functional specialization of different parts of the body, contributed to the successful diversification of annelids. Differences along the body axis are expressed in the arrangement of chaetae, parapodia (lateral outgrowths of the body), coelomic cavities and coelomoducts, musculature, and the nervous system (5–7). These differences are already evident in several early branching lineages of annelids, such as Oweniidae, Mageloniidae, Psammodrilidae, and Chaetopteridae(8–14). The recently discovered Cambrian endobentic magelonid-like annelid *Dannychaetae* also possess a heteronomously segmented body (Chen et al., 2020). The phylogenetic position and old origin of these annelid taxa urge for new comparative analyses and ancestral reconstruction of segmental organisation in annelids, which might not have been homonomous as previously suggested (15–18). Developmental studies of heteronomous representatives are therefore essential for identifying possible common formation schemes across annelids and reconstruct the evolution of segmental organization in Annelida.

The iconic family of deep-sea gutless worms, Siboglinidae, has a heteronomous body architecture. Siboglinids are found in reducing habitats, and includes Vestimentifera (hydrothermal vents and hydrocarbon seeps), *Sclerolinum* (sediments, and decaying organic matter), *Osedax* (from the decaying vertebrate bones, and sediment beneath), and Frenulata (from seeps and sediment enriched with sulphides) (19–23). Siboglinidae are nested within Sedentaria in Pleistoannelida (8, 9). Within Siboglinidae, the frenulate pogonophorans constitute the sister clade to the remaining siboglinids (24). The frenulates are characterised by the presence of a small cephalic lobe, a forepart bearing frenulum and tentacle, a highly elongated trunk (encompassing maturing gametes and endosymbiotic bacteria), and an opisthosome, with chaetae-bearing short segments. However, for a long time siboglinids were considered as deuterostomes, consisting of three body parts (25, 26), and only in the nineties did molecular based analyses finally place them within Annelida (e.g., (27)). Detailed comparative analyses of the body plan of frenulate pogonophorans and other annelid clades that demonstrate a heteronomous body plan have not yet been carried out.

Current knowledge on the anatomy of siboglinid larvae is mainly based on ultrastructural studies of vestimentiferans (28–32), and immunolabeling and confocal scanning microscopy on larva-like male of *Osedax* (33). Only few histological(34–36) and ultrastructural(37) data on frenulate larvae exist and their full anatomy needs to be reconstructed with advanced microscopy techniques and considering their current position within Annelida.

Frenulate pogonophorans, forming a sister clade to the remaining siboglinids, provide an excellent model for studying heteronomous development in this group. We have focused on muscle development, which as mesodermal tissue set the segment borders prior to the appearance of ectodermal borders (38–42). The myogenesis of *Siboglinum fiordicum* is mapped and reconstructed with F-actin (phalloidin) staining and confocal laser scanning microscopy and ultrastructural details investigated employing transmission electron microscopy. The structure and development of musculature and septa shed light on the regionalization of the body and temporal formation of segments along the anterior-posterior axis.

Videorecording of live animals provides information on larval motility patterns that in combination with the morphological data allow us to hypothesize on the functional adaptation to the larval lifestyle of the of frenulate pogonophorans, and particularly *Siboglinum fiordicum*.

Results

General description of larvae stages

To study the development of muscles in *Siboglinum fiordicum*, we reconstructed the muscular architecture and anatomy in four successive stages: trochophora, early metatrochophora, late metatrochophora, and competent larva (Figs. 1–5).

The size and shape of the trochophores are comparable to those of the eggs. The widest part of the larva is in the middle of the body (Figs. 1A-C). The trochophore larva has a small convex episphere (*esp*) (without an apical tuft of cilia) and an unusually long hyposphere (*hsp*). The earliest trochophore stage have a thin, irregular prototroch (*p*). In late trochophores, an irregular strip of mesotroch (*m*) appears (Fig. 1C), and a wide prototroch is formed by large multicilated trochoblast cells (*mbl*) arranged in 2–3 rows (Figs. 1B-C, 2A-B, 3A).

The early metatrochophora has a wide prototroch, represented by first short (Fig. 2A), then longer cilia (Fig. 2B) of similar length (there are no opposed beating cilia). The mesotroch becomes a regular annular stripe (Fig. 2A) with cilia soon extending length and density (Fig. 2B), and a neurotroch and a dorsal ciliary spot (*cp*) appear (Figs. 2A, B). The neurotroch is a wide ventral ciliary field, consisting of two zones, a small anterior (*na*) and a larger posterior (*np*) (Fig. 2A). At this stage, the chaetae of the annula (*ca*) (middle part of “trunk” or 3rd segment) and the chaetae of the first segment of the opisthosoma (*co*) (i.e., the 4th body segment) are laid under the epidermis (Figs. 2C-H). The chaetae are not visible externally, but scanning electron micrographs show depressions of the future chaetae of the opisthosoma (Fig. 2B).

Late metatrochophores of *S. fiordicum* are noticeably elongated. In the cone-shaped prostomium (*pr*) of the larva, a frontal fold (*aff*) appears on the ventral side (Fig. 3A). The peristomium (*pe*), located behind the prototroch, carries a tentacle rudiment (*tb*), which is laid on the dorsal side to the left of the ciliary spot (Fig. 3B). *S. fiordicum* does not have a mouth opening, but a gap in the musculature (Fig. 3F’). The second segment bears a neurotroch, comprising an anterior and a posterior zone. The third segment of the larva (the trunk of adult pogonophorans) is a narrow part of the body, located posterior to the middle fold of the body and stretching to the first septum which borders the anterior segment of the opisthosoma (Fig. 3A). In the first segment of the opisthosoma, large chaetae are clearly visible and a thin mesotroch posterior to the chaetae (Fig. 3a).

In the competent larva, the prototroch almost disappears. In the peristomium, there is an anlage of tentacle and a dorsal ciliary spot. In the second segment (“forepart segment” in adult frenulates), the frenulum (*f*), or bridle, appears. The third segment (trunk segment of adult frenulates) is delineated anteriorly and posteriorly by septa (*s1*), and in the middle part, chaetae of the annula, extend externally

(Fig. 4A). The first segment of the opisthosoma, between the first septum and the mesotroch, is relatively long. In the relaxed larvae, this segment exceeds the length of all subsequent segments of the opisthosoma (Figs. 4A-E).

Phalloidin staining results. General description. The somatic musculature is formed at the early metatrochophore stage and is represented by layers of longitudinal and circular muscles (Figs. 2–5). The longitudinal musculature comprise four separate strands located ventrally (*mv*), dorsally (*md*), and ventro-laterally (*mvl*). The circular muscles (*mc*) are evenly distributed as complete wide bands along the body of the larvae from the apical end to the annular chaetae. From the annular chaetae to the first septum, there is a body region (future trunk segment) devoid of the circular muscles and longitudinal muscles constricted into four bundles. The bundles of longitudinal muscles form the first septum separating the trunk segment from the first segment of the opisthosoma (Fig. 6). In the opisthosoma, posterior to the first septum, the circular muscles are organized in distinctly separate bundles (Figs. 2–6). In the larvae, the musculature of the future tubiparous glands is laid, as well as the muscular apparatus that controls the movement of the opisthosomal chaetae (Figs. 2E-H, 7, 8).

Longitudinal musculature. Four main longitudinal muscle strands extend from the prostomium to the posterior end of the opisthosome in the larvae: one ventral (*mv*), one dorsal (*md*), and two ventro-lateral (*mvl*).

The dorsal (*md*) and ventral (*mv*) longitudinal strands are unpaired for the most of their length. The ventral strand is the narrowest. The widest strands are the ventro-lateral ones, which have two longitudinal components at all studied larval stages: ventral (*mvvl*) and lateral (*mlvl*). The ventral component (*mvvl*) originate at the anterior prototroch and insert at the posteriormost body, while the lateral component (*mlvl*) originate at the anterior prostomium and insert at the first septum.

The number of bundles in each muscle strand remains unchanged from the prostomium to the posterior end of the opisthosoma. But the number of fine fibers that make up the bundles varies. For example, the dorsal muscle strand (*md*) is formed as a single wide strand, which bears about 8–9 bundles in all stages (Figs. 2–5). The number of bundles within a strand does not change with age, but the thickness of each bundle changes due to the increasing number of muscle fibers that make up the individual bundles.

At the early stage of formation, the fibers of the longitudinal muscles are grouped in separate bundles (Figs. 2C-E), while at the later stages of development, the fibers form a continuous muscle layer (Figs. 3C, D, 4D, E). For example, in the trunk segment (3rd segment), the longitudinal fibers of all four muscle strands run widely so that they almost form a continuous layer of longitudinal muscles (here the longitudinal strands are interconnected by short lateral circular muscle fibers (*mcc*) (Figs. 3C, D, 4C, D). In the posterior trunk, the longitudinal muscle fibers are grouped into dense bundles. The muscle fibers that are grouped into bundles in the posterior part of the trunk segment have a similar pattern in all studied samples: the dorsal strand is represented by two bundles (md1-2), the ventral one - by one bundle, and the ventro-lateral muscle strand is represented by three (mvvl1-3) and two (mlvl1-2).

At the stage of late metatrochophora, in the area of the potential temporary mouth anlagen, the bundles of the ventral longitudinal muscle strand split (Fig. 3F'). At an earlier and later stage, this hole is not visible.

Circular musculature. The circular musculature forms a muscular dense corset in the anterior part of the larva (Figs. 2, 3, 4, 5). From the apical end till the anterior trunk segment, the circular muscle fibres are distributed as wide bands, surrounding the larval body. Each band includes about eight complete circular muscle bundles. Under the prototroch, the bundles are semi-circular and overlap mid-dorsally and mid-ventrally (Figs. 2C, D', 3F', 4E). On the dorsal side posterior to the prototroch, the circular muscles form two slightly asymmetrical holes (Fig. 2C). The left hole corresponds to the future unpaired tentacle (*tm*). In the later stages (competent larva), a muscle ring appears at the base of the tentacular anlage (Figs. 4C, D, 5I).

In the trunk segment of the early metatrochophore, the circular bands are sparsely located (Figs. 2C, 3B, 4C, 5G-I). Later, the trunk segment lengthens and forms two parts. In the anterior part (until to the annular chaetae), 4–5 circular bundles are visible, and in the posterior part of the body (behind the annular chaetae), there are no circular muscles at all.

Septal musculature and sequence of their formation. The first septum (*sI*) divides the body of the early metatrochophora into two parts: an anterior segment and a posterior opisthosomal segment (Figs. 4, 5). The formation of the first septum completes already in the late metatrochophora, which encompass the closure of the ecm layer and the formation of a continuous layer of longitudinal muscles (Figs. 6, 11). The formation of specialized longitudinal musculature along the lateral sides of the first opisthosomal segment accompanies the development of the first septum between the trunk segment and the first segment of the opisthosoma. The bundles of this musculature are laid down at the stage of the early metatrochophore and gradually grow in thickness at later stages. The first septum is based on a layer of extracellular matrix, which gradually deepens from the body wall into the body of the larva. In early metatrochophora, the septum is incomplete, there is a lumen in the middle of the septum, through which the larval intestine runs. At later stage, the edges of the extracellular matrix of the septum join, and the septum completely separates the trunk segment and the opisthosoma. Following this, the longitudinal muscle bundles of the septum also transverse deep into the body. In the late stages, the longitudinal musculature extends from the first septum till the second septum of the opisthosoma. There are ca 24 pairs of longitudinal bundles building the first septum. With the larval development the bundles significantly increase in length (Figs. 2F, 6). Ca 12 large myoepithelial cells with large nuclei (*mcn*) form this septal muscle (Figs. 6D, 9A).

At the late metatrochophore stage, three more separate circular bands are added at the posterior end of the opisthosoma (Figs. 3C, F). Subsequent septa (*sII*) form posterior to the first septum, splitting the opisthosoma into additional segments. There is an outstripping development of circular muscle bands, which seem to outline the boundaries of the opisthosomal segments, followed by the development of muscle-less inner septal divisions (Figs. 2F-H, D, 5I, 11). In the early metatrochophora, three circular bands

are formed (Figs. 2C, F): the first at the level of the first pair of chaetae, the second beneath the mesotroch. The third is located posterior to the second one. The early metatrochophora has these three opisthosomal circular muscle bands but no internal septa yet (Figs. 2E-H), while the late metatrochophora already has six opisthosomal circular muscle bands and six septa (Figs. 3C, F).

At the stage of the competent larva, a distinct circular muscle bands (*mf*) is visible in the middle of the anterior body segment. We assume these muscles correlate to the position of the anterior septum (*sIII*) which divides the anterior body segment into two segments (forepart and trunk) (Fig. 4A, C, E). These two segments (following the peristomium or 1st segment) grow without further divisions into the adult stage. The anterior segment is termed the forepart (following Southward (43)), which is equivalent to the "fused protosome and mesosome", according to the now abandoned deuterostomic concept of Ivanov (44). The posterior segment is termed the trunk (following Southward (43)) and is equivalent to the "metasome", according to the now abandoned deuterostomic concept of Ivanov (44)). In this second body segment (forepart) there is a frenulum (or bridle, a characteristic structure found in all the currently described frenulates (see, for example, Ivanov (26); Southward et al. (45)), and in the third segment (trunk) there are annular chaetae that detach the preannular (genital) and postannular (trophosomal) parts. The following circular bands and septa are formed at the very end of the opisthosoma one by one; For example, at the stage of the competent larva, a seventh circular band forms (Fig. 4H). Later in the post-larval stages a new circle band and a new segment form at the very posterior end of the juvenile. Adults of *S. fiordicum* have up to 21 muscle septa in the opisthosoma (unpublished data) Within the circular opisthosomal bands, number of fibers increases with the age of larva. For example, from 7 to 12 fibers within the bundle located under the mesotroch (Figs. 2F, 4H).

Musculature of chaetae. The movement of the chaetae of the first segment of the opisthosoma is controlled by both specialized chaetal muscles and somatic muscle bundles. The latter include the longitudinal septal musculature (*mls*) and the circular septal musculature (*moc1*) (Fig. 7, 8). The chaetal muscles include separate circular and longitudinal muscle bundles. In total, there are 3 circular muscle bundles (*mcch1-3*) and about 10 longitudinal muscle bundles (*mlch1-10*) for each pair of chaetae (Figs. 2F-H, 7, 8). The circular muscles of the chaetal apparatus lie in the ventro-lateral and dorso-lateral directions (*mcch1-3*). Among the circular muscles, the first one (*mcch1*) stands out, one end reaching the ventral cord of the longitudinal muscles (mv), and the other attaching the body wall at the level of the septal muscles (*mls*) (Figs. 7A, 8). The first circular muscle lies at the base of the chaetae in such a way that the ends of the chaetae "abut against it". This circular muscle serves also as an anchor for almost all longitudinal muscles of the chaetae apparatus (*mlch1-4, 6–10*) (Figs. 7A-D). The rest of the circular chaetal muscles originate at the ventral longitudinal cord and supply the distal ends of the chaetae.

The longitudinal muscles of the chaetal apparatus attach with their distal end to the body wall either at the level of the first segment (*mlch1-6*) or at the level of the second segment (*mlch7-10*). The proximal end of the longitudinal chaetal muscles anchors either on the chaetae (*mlch5*) or on the first circular muscle or in the immediate vicinity of it (*mlch1-4, 6–10*) (Figs. 7A-D).

The annular chaetae (*ca*) at the stage of the competent larva are not yet fully formed; therefore, we assume that the musculature is not yet fully formed. At the studied stages, we see that the four pairs of annular chaetae are controlled by their own muscles, which includes a pair of circular bundles (*mca*) and longitudinal bundles that extend from the ventrolateral longitudinal muscle strands (*mvl*) (Figs. 2G, 3B, 4G).

Musculature of tubiparous glands. Phalloidin stained the muscular sheaths of the sacs and ducts (*mtg*) of tubiparous glands in larvae, from the early metatrochophora to the competent larva (Figs. 2E, 3F, 4D-E). At all stages, they are located in the posterior half of the anterior part, throughout the entire trunk segment, and in the first segment of the opisthosoma (Figs. 2E, 3C, 4G). Moreover, the tubiparous glands are associated with radial muscle bundles (*mrtg*) extended from the somatic longitudinal strands to the distal portion on the gland (Figs. 2E, 4C).

Ultrastructure. In general, the somatic musculature is formed by myoepithelial cells of the coelomic lining. These are large cells with a prominent apical part and large basal projections (Figs. 9A, 10A). Cells connect via adherence junctions (*aj*) which are located at the border between the apical part of cell and the basal projections and also on the membranes of muscular projections (Figs. 9A, 10A). The apical part of the cell bears large irregular-shaped nucleus containing a few amounts of condensed chromatin and large nucleolus (Figs. 9A, 10A). Cytoplasm around nucleus is filled with numerous mitochondria of small diameter and electron dense matrix, canals of rough endoplasmic reticulum (*re*), and inclusions of different types. Basal projections of myoepithelial cells abut on the thin layer of extracellular matrix (*ecm*), which is highly electron dense (Fig. 9B). In some places, which are probably able to stretch extensively, the basal membrane of the muscular projections forms numerous finger-like outgrowths (*flo*), which repeat the folds of extracellular matrix and epithelium of body wall (Fisg. 9A, 10A). The cytoplasm of muscular projections is filled with numerous myofilaments, which mostly extend in longitudinal direction (Fig. 9B) but can also extend at the angle to the body wall (Fig. 9A, 10B). Myofilaments connect the basal membrane to cell via electron dense hemidesmosomes (*he*) (Fig. 10C). Myofilaments are organized as in cross-striated musculature: there are sarcomeres (*sa*) and Z-bodies (*Zn*) (Fig. 10B). Cytoplasm of muscular projections contains mitochondria of small diameter and a few electron dense inclusions (Fig. 10A).

In the somatic longitudinal muscle strands, several myoepithelial cells connect and form a pseudo-multilayer (Fig. 10A). This construction forms because muscular projections of cells overlay each other. However, all cells contact the layer of extracellular matrix and, hereby, myoepithelial cells form the monolayer (Fig. 10A). In some places where the myoepithelial cells and their projections contact each other, the cell membranes form numerous finger-like protrusions, which all together work as interdigitate cell junction (Fig. 10D).

In septa, the myoepithelial cells have large apical part that extend into coelom lumen of the 1st opisthosomal segment and contains large nucleus in basal parts (Figs. 11A, B). These cells connect not only *via* adherence junctions, but also by septate junction (Figs. 11B, B'). Muscular projections of cells

extend in radial direction, i.e., from body wall to the center of the septum, at a right angle to anterior-posterior body axis (Figs. 11A-C).

According to CLSM, the tubiparous glands are associated with radial muscle bundles (*mrtg*), which extend between dorsal and ventrolateral longitudinal muscles strands and distal portion on the gland (Fig. 2E, 4C). Cells of the radial muscles directly abut on the cells of gland lumen (Fig. 11D). The contraction of radial muscles promotes the extrusion of the secret from the lumen of the gland to environment.

The complicated musculature of the chaetal sacs is organized by the myoepithelial cells (Fig. 12A). All cells are connected *via* adherence junctions and have large muscular projections (Fig. 12B). Some of myoepithelial cells form the circular muscle lining, which envelopes the follicle cells and chaetae (*co*) (Fig. 12B). Other cells form the longitudinal muscles of chaetal sac (Fig. 12C). These cells extend between the layers of extracellular matrix of the chaetal sac and the epithelium of the body wall. On both sides, the myofilaments adhere to the extracellular matrix *via* hemidesmosomes. Myofilaments are mostly passed in a longitudinal direction. Interestingly, myofilaments are attached peripherally to the extracellular matrix exactly where the thick bundles of electron dense tonofilaments (*tf*) of epithelial cells are attached on the opposite side of the ecm basal membrane. These tonofilaments extend into tips of microvilli and attach to the cuticle (Fig. 12C). Thus, the myofilaments of the longitudinal muscles of the chaetal sac indirectly attach to the cuticle via thick tonofilaments of the epidermal cells.

During observations of the larvae, we have recorded videos on the characteristic movement of the larvae at each of the stages of development described in the work. Examples of detailed movements can be seen in the videofile, Additional file 1. Trochophores float due to the beating of cilia, their body does not bend. They actively swim out of the maternal tube and can spin and swim on the bottom of the dishes. Metatrochophores still actively swim using cilia, but they bend the body, so that their swimming can be accompanied by rotational movements. Late metatrochophores stop actively swimming, they often lie at the bottom of the glass dish or sediment but continue to bend the body. Chaetae are often anchored in the sediment particles. Competent larvae burrow into the sediment head downward, their rotating posterior end of the body is visible outside the sediment.

Discussion

Mesotroch. We define the posterior ciliary band in frenulate *Siboglinum* as a mesotroch following the definition of Irvine et al. (46) and Rouse and Plejel (4). According to the authors, mesotrochs are large and complete circular ciliary bands that eventually come to lie within the segmented body. This fact makes mesotroch different from the metatroch and telotroch. This band should not be termed a paratroch, which forms after the formation of the telotroch around the segments, for example in nereidid larva (47, 48). As a result, if we call this ciliary band in *Siboglinum* as "mesotroch", then we expand the term of (49), which considers that prototroch and telotroch in mesotrochal larvae completely degenerate.

Larval movement. The somatic muscles are responsible for the generalized movement of the larva's body. The strands of the longitudinal muscles provide bending of the larva's body in various directions relative to the longitudinal axis. The development of a longitudinal layer of musculature in the trunk and in the opisthosoma of the late larvae indicates a special role of the posterior half of the larva's body in generating body movement, including burrowing into sediment. The circular musculature, as an antagonist of the longitudinal musculature, provides the elongation of the larva's body along the longitudinal axis. The significant development of a continuous layer of circular muscle in the anterior half of the body indicates that this end is intensely shrinking and stretching along the longitudinal axis, which is important for successful penetration into the sediment. The muscular apparatus of the chaetae of the opisthosoma is complexly organized, which suggests a special role of these chaetae in the mobility of the body of the larvae, having a near-bottom lifestyle.

In swimming metatrochophores, there is a wide neurotroch, which presumably serves as a sense organ and for ciliary gliding, thus the ventro-lateral longitudinal muscle strand and allow to produce “exploratory” or “search” side to side movements. The strands of the longitudinal muscles provide bending of the larva's body in various directions along the longitudinal axis. The positions and widths of the longitudinal muscle strands indicate that the larvae may bend mainly dorsally and ventrally due to the widest dorsal longitudinal strand and joint work of ventrolateral and ventral longitudinal strands. This undulatory body wave-movements might help them to crawl or burrow into sediment.

Particularly intensive muscle development is the “preannular” area of the trunk segment (the area of the body anterior to the annular chaetae), which makes about ¼ of the total length of the larva, and the longitudinal muscles of the first septum of the opisthosoma. At the late larval stages (Fig. 3, 4), the longitudinal muscles in the preannular area are so developed that they cover almost the entire perimeter except for narrow gaps. Most of this muscle "corset" is made up of the dorsal and ventrolateral strands, the ventral strand is still less developed. A solid layer of musculature in this area and the intensive development of the longitudinal muscles of the first septum of the opisthosoma may indicate that the posterior part of the body actively moves at the late larval stages, providing intensive rotation of the posterior end of the body and repulsion of the larva. Larvae can crawl towards the anterior end of the maternal tube or over the sediment by pushing the posterior end of the body in all directions. These muscles are indirectly involved in the movement of the opisthosomal chaetae which facilitate anchoring or are involved in the process of burying the larva in the sediment.

It seems to us that the unusual observed rotational movements of the larval are reflected in the unusual organization of the longitudinal strands of the frenulates: there is one dorsal and one ventral and two ventrolateral strands of the longitudinal muscles, while the more popular position of the longitudinal bundles in annelids is pairs of dorsal and ventral ones (15, 50).

Circular muscles are likely more important for burrowing forms, but not required for animals that move through parapodial movements or cilia (50). This explains why the anterior end of the *Siboglinum* larvae, equipped with a continuous layer of circular muscles, is specialized to burrow into sediment using

peristalsis (51). But a distinctive feature of the *Siboglinum* larvae is that the circular muscles are seemingly located within or internal to the longitudinal muscles (Fig. 9B). It is not yet clear what advantage this gives *Siboglinum* and other annelids such as *Sphaerodoropsis* (Sphaerodoridae) and *Lobatocerebrum* (52–54).

Chaetal movement. Annular chaetae do not function in the studied larval stages; adult frenulates use them to attach to the tube. At the late larval stages, 4 pairs of chaetae of the first segment of the opisthosoma are very mobile (an additional movie file shows this in more detail, see Additional file 1), and their movement is carried out by a set of longitudinal and circular muscle bands (Fig. 7, 8). From the muscular reconstructions we suggest the following functionality of the various muscles: each pair is located in a single chaetal sac and the “neighbors” are controlled by the muscle bundles synchronously (Fig. 12). The first annular muscle (mcch1) serves as an anchor for almost all longitudinal bundles of the chaetal apparatus (except mlch5). The longitudinal bundles (mlch1-10) provide forward and backward movement of the chaetae, but their joint work with mcch1 provides rotational movements of the chaetae. Longitudinal bundles having an anterior position (mlch1-4) provide backward movement of the chaetae, the mlch5 bundle attached to the chaetae and mlch6 bundle move the chaetae dorsally and slightly forward. The longitudinal muscles, which have a posterior attachment to the body wall (mlch7-10), serve as levers to move the chaetae forward. Mlch7-8 move the setae forward and dorsally, while mlch9-10 move forward and ventrally. The circular muscles mcch2-3 are responsible for the retraction and descent of the chaetae, pressing them against the longitudinal axis of the body and decreasing the angle with the longitudinal axis.

Sequence of septa formation and regionalization of the body. In the frenulate larva the border between the prostomium and the peristomium, bearing the ventral mouth and dorsal tentacle, is distinguishable and the regionalization follows that of other annelid larvae (37, 55). But the division of the rest of the body raised questions (32, 56).

The division of the *Siboglinum* body into segments does not occur in a strict direction from posterior to anterior end, but in an altered order. Posterior to the first muscle septum (SI), six non-muscular septa (SII) are formed simultaneously in the opisthosoma, followed by the formation of the anterior body septum (SIII), which separates the forepart from the trunk in adult frenulates. Thereafter, further segments emerge sequentially at the end of the opisthosoma. According to the classical concepts of annelid development, after the simultaneous formation of the larval segments, the next segments are sequentially added from the posterior growth zone (5, 57–59). This is well studied in errant nereid with the homonomous body plan *Platynereis dumerili* (1, 2). But in *S. fiordicum* with the heteronomous body plan, we do not observe a distinct posterior-anterior sequence of segment formation.

Instead, the first septum in *Siboglinum* divides the body into two tagmas, and later the segmentation occurs within the tagmas. In very similar way, the formation of segments in the heteronomous chaetopterid *Chaetopterus variopedatus* occurs within the body tagmas, in an altered order, not strictly from posterior to anterior (46). The absence of the postero-anterior sequence of the anlage of segments

is also known in other sessile annelids, for example heteronomous annelids *Capitella teleata* and *Hydroides elegans* from the group of Sedentaria (60). Sessile myzostomids and sipunculids also build their body without a distinct posterior growth zone (61, 62). This makes us speculate whether a posterior growth zone and a clear postero-anterior growth pattern may not be the norm in Annelida and possibly neither the ancestral mode of development in Annelida. In *Siboglinum fiordicum*, we furthermore suggest that its segmental formation associates to the characteristics of the life cycle and ecological adaptations of the larvae. The first to appear are the opisthosomal segments at the posterior end of the larva, which is associated with the mobility of the posterior end of the larva's body necessary for emergence from the mother tube and for subsequent burying of the larva in the sediment (burying of the larva in the sediment is described in Bakke (51)).

Conclusions

Our results show that septa formation in the *Siboglinum fiordicum* did not follow a strict temporal anterior to posterior sequence described as the ground pattern in annelids. Instead, the first septum divides the body into two regions (tagmas). Later the segments lay down within these regions: first posteriorly in the opisthosomal segment, later anteriorly in the anterior segment. We consider larvae of *S. fiordicum* as heterochronous, in that segments in each of the body tagmas develop at different times and rates rather than the more typical homochronous pattern found in other annelids where septa formation during larval development follows an anterior-posterior temporal sequence. Heterochronous larval development has likely evolved together with the heteronomy (specialized body regions) in adult body form found in *S. fiordicum*. Growth patterns lacking a strict anterior-posterior sequence of segment formation are found in different genera including *Capitella, Hydroides, Chaetopterus*, and myzostomids. They contrast classical studies of annelid development showing that segmented annelids usually generate their first (three) larval segments simultaneously while later segments are sequentially added from a posterior growth zone, e.g. in *P. dumerilii*. Based on the position of heteronomous annelids in phylogenomic studies, and also based on the fact that the recently discovered Cambrian fossils of a heteronomous annelid is the earliest annelid discovered so far, we put forward a hypothesis: that heteronomous segmentation in annelids might date back to the earliest Annelida, although likely convergently evolved multiple times during the evolution of Annelida.

Methods

Specimens of *S. fiordicum* were collected at 18–35 m in the Ypsesund Strait (North Sea) in the close vicinity of the Espegrend Marine Biological Station, University of Bergen, Norway. Later in the lab, larvae were extracted from female tubes.

Scanning electron microscopy **(SEM)**. Larvae were anesthetized with 7% MgCl2, were fixed in 2,5% glutaraldehyde in 0,1M cacodylate buffer with 5% sucrose and later postfixed in 1% osmium for 1,5 hours, dehydrated, dried out at the critical point and sputter coated with a platinum. SEM studies were

performed on the JEOL JSM microscopes (JEOL Ltd., Tokyo, Japan) at the Laboratory of Electron Microscopy of Moscow State University.

Confocal laser scanning microscopy (CLSM). Larvae were anesthetized with 7% MgCl2, fixed with 4% paraformaldehyde over nigth at 4°C and then rinsed six times in phosphate-buffered saline (PBS). After 1 h preincubation in PTA (PBS + 5%Triton, 0,05%NaN3 and 0.25% BSA) animals were stained for 1 h with Alexa Fluor 488-labeled phalloidin (INVITROGEN, Carlsbad, USA) dissolved in PTA, to visualize F-actin. For cilia visualization the monoclonal mouse acetylated α-tubulin (final concentration 1:400; Sigma-Aldrich, T6793) was used (with CY5 labeled secondary antibody directed against mouse; Jackson Immuno-Research, West Grove, PA, USA). Samples were preincubated for 1–2 hours in PTA (PBS + 5% Triton-X, 0.05% NaN3, 0.25% bovine serum albumin, and 10% sucrose). Afterwards, samples were incubated for up to 48 hours at RT in the primary antibody, both made with PTA (with 1% Triton). The samples were then thoroughly washed through several shifts with PTA over 6 hours and then incubated overnight at RT in the two respective secondary antibodies conjugated with fluorochromes and mixed in PTA. Stained animals were mounted in Vectashield® Antifade Mounting Medium with DAPI (Vector Laboratories, Burlingame, CA, USA) and examined with Olympus Fluoview FV-1000 confocal laser scanning microscope (CLSM) in the University of Copenhagen. Z stacks of scans were projected into 2D-images and 3D reconstructions in Fiji and AMIRA 2020 (ThermoFischer Scientific) and used for shematic drawings made in Adobe Illustrator 2020. CLSM images were adjusted in Adobe Photoshop 2020 and assembled in Adobe Illustrator 2020.

Ultrastructure studies. Specimens were fixed in 2,5% glutaraldehyde in 0,1M cacodylate buffer with 5% sucrose and later postfixed in 1% osmium for 1,5 hours. Prior to embedding in Spurr, specimens were dehydrated in alcohol series using standard protocol and thereafter polymerized for 20–24 hours at 60°C. The block was trimmed to the object and sectioned into semithin (500 nm) and ultrathin (30–40 nm) sections using a Leica EM UC7 ultramicrotome (LEICA MICROSYSTEMS, Wetzlar, Germany). Ultrathin sections were mounted on slot grids and mesh grids, contrasted with 1% uranyl acetate- and 4% lead citrate-solution. Transmission electron microscopy (TEM) performed with JEOL JEM-1011 equipped with digital camera ORIUS SC1000W, and JEOL JEM-1400 Flash equipped with Gatan Rio 9 fast CMOS 3k camera (JEOL Ltd., Tokyo, Japan) at the Laboratory of Electron Microscopy of Moscow State University. Later pictures were processed in Adobe Photoshop 2020 and assembled in Adobe Illustrator 2020.

Videorecordings. To make a video, an iPhone 6S smartphone (Apple Inc.) and an iDu CamLab adapter (iDu Optics, USA) for a stereomicroscope on an iPhone are used. Video processing was done in Adobe Premiere Pro CS6 (Adobe Systems Incorporated, San-Jose, USA, 2012).

Declarations

Ethics approval and consent to participate

Not applicable

Consent for publication

Not applicable

Availability of data and materials

All data (electron and confocal microphotographs, movies, and schemes) are kept by NRK and available by personal request.

Competing interests

The authors declare that they have no competing interests.

Funding

The study was partly supported by the Russian Foundation for Basic Research project № 18-34-20140 (sampling, CLSM, and SEM, studies) and the Russian Science Foundation, project № 20-74-10011 (TEM studies and processing of the paper). The research was carried out as part of the Scientific Project of the State Order of the Government of Russian Federation to Lomonosov Moscow State University No. 121032300121-0. CLSM work was supported by the Carlsberg Foundation (grant # CF15-0946).

Authors' contributions

NNRK, KW and ENT designed the study. All authors except ENT participated in sampling and fixation of the material. NRK, KW, NK, and ENT performed the experiments; NRK, ENT, NK analyzed the data, made the illustrations and drafted the manuscript. All authors corrected and approved the final version of the manuscript.

Acknowledgements

We greatly acknowledge Nataliya Budaeva and our colleagues from the University of Bergen for the sampling opportunity at the Espegrend Marine Biological Station, as well as station staff and especially Tomas Knut Sorelie for sampling the *S. fiordicum* specimens in the vicinity of the station. We thank the staff of the Cooperative Laboratory of Electron Microscopy of Lomonosov Moscow State University for providing TEM and SEM facilities.

Authors' information (optional)

Not applicable

References

1. Balavoine G. Evolutionary developmental biology and its contribution to a new synthetic theory. In: Handbook of Evolutionary Thinking in the Sciences. Springer Netherlands; 2015. p. 443–70.

2. Özpolat BD, Handberg-Thorsager M, Vervoort M, Balavoine G. Cell lineage and cell cycling analyses of the 4d micromere using live imaging in the marine annelid Platynereis dumerilii. eLife [Internet]. 2017 Dec 12;6. Available from: https://elifesciences.org/articles/30463
3. Goodrich ES. Memoir: The study of Nephridia and genital ducts since 1895. Journal of Cell Science. 1945;2(342):113–301.
4. Rouse G, Pleijel F. Polychaetes. Oxford university press; 2001.
5. Koch M, Quast B, Bartolomaeus T. Coeloms and nephridia in annelids and arthropods. In: Wägele JW, Bartolomaeus T, editors. Deep metazoan phylogeny: The backbone of the tree of life . De Gruyter; 2014. p. 173–284.
6. Bleidorn C, Helm C, Weigert A, Aguado MT. Annelida. In: Evolutionary developmental biology of invertebrates 2. Springer; 2015. p. 193–230.
7. Purschke G. 24 Annelida: basal groups and Pleistoannelida. Structure and evolution of invertebrate nervous systems. 2015;254.
8. Struck TH, Paul C, Hill N, Hartmann S, Hösel C, Kube M, et al. Phylogenomic analyses unravel annelid evolution. Nature. 2011;471(7336):95–8.
9. Andrade SCS, Novo M, Kawauchi GY, Worsaae K, Pleijel F, Giribet G, et al. Articulating “archiannelids”: Phylogenomics and annelid relationships, with emphasis on meiofaunal taxa. Molecular Biology and Evolution. 2015;32(11):2860–75.
10. Weigert A, Bleidorn C. Current status of annelid phylogeny. Organisms Diversity & Evolution. 2016;16(2):345–62.
11. Rimskaya-Korsakova NN, Kristof A, Malakhov V v, Wanninger A. Neural architecture of Galathowenia oculata Zach, 1923 (Oweniidae, Annelida). Frontiers in zoology. 2016;13(1):1–19.
12. Helm C, Vöcking O, Kourtesis I, Hausen H. Owenia fusiformis–a basally branching annelid suitable for studying ancestral features of annelid neural development. BMC evolutionary biology. 2016;16(1):1–19.
13. Helm C, Beckers P, Bartolomaeus T, Drukewitz SH, Kourtesis I, Weigert A, et al. Convergent evolution of the ladder-like ventral nerve cord in Annelida. Frontiers in Zoology. 2018 Sep 27;15(1).
14. Worsaae K, Giribet G, Mart\’\inez A. The role of progenesis in the diversification of the interstitial annelid lineage Psammodrilidae. Invertebrate Systematics. 2018;32(4):774–93.
15. Clark RB. On the structure and functions of polychaete septa. In: Proceedings of the Zoological Society of London. 1962. p. 543–78.
16. Westheide W. The direction of evolution within the Polychaeta. Journal of Natural History. 1997;31(1):1–15.
17. Purschke G. On the ground pattern of Annelida. Organisms Diversity & Evolution. 2002;2(3):181–96.
18. Arendt D. Spiralians in the limelight [Internet]. Vol. 4, Genome Biology. 2003. Available from: http://genomebiology.com/2003/5/1/303

19. Bright M, Lallier FH. The biology of vestimentiferan tubeworms. Oceanogr Mar Biol Annu Rev . 2010; 48:213–66.
20. Georgieva MN, Wiklund H, Bell JB, Eilertsen MH, Mills RA, Little CTS, et al. A chemosynthetic weed: the tubeworm Sclerolinum contortum is a bipolar, cosmopolitan species. BMC Evolutionary Biology. 2015;15(1):1–17.
21. Rouse GW, Goffredi SK, Johnson SB, Vrijenhoek RC. An inordinate fondness for Osedax (Siboglinidae: Annelida): Fourteen new species of bone worms from California. Zootaxa. 2018 Feb 5;4377(4):451–89.
22. Karaseva N, Gantsevich M, Obzhirov A, Shakirov R, Starovoitov A, Smirnov R, et al. Correlation of the siboglinid (Annelida: Siboglinidae) distribution to higher concentrations of hydrocarbons in the Sea of Okhotsk. Vol. 158, Marine Pollution Bulletin. Elsevier Ltd; 2020.
23. Karaseva NP, Rimskaya-Korsakova NN, Ekimova IA, Gantsevich MM, Kokarev VN, Kremnyov S v., et al. A new genus of frenulates (Annelida: Siboglinidae) from shallow waters of Yenisey river estuary in the Kara Sea. in press.; 2021.
24. Li Y, Kocot KM, Whelan N v, Santos SR, Waits DS, Thornhill DJ, et al. Phylogenomics of tubeworms (Siboglinidae, Annelida) and comparative performance of different reconstruction methods. Zoologica Scripta. 2017;46(2):200–13.
25. Beklemishev VN. Osnovy sravnitelnoi anatomii bespozvonochnykh h (Fundamentals of Comparative Anatomy of Invertebrates) (in russian). 1st ed. Moscow: Sovetskaia nauka; 1944. 1–492.
26. Ivanov AV. Pogonophora. Carlisle DB, editor. London: Academic Press; 1963. 1–479.
27. McHugh D. Molecular evidence that echiurans and pogonophorans are derived annelids. Proceedings of the National Academy of Sciences. 1997;94(15):8006–9.
28. Southward EC. Development of the gut and segmentation of newly settled stages of Ridgeia (Vestimentifera): implications for relationship between Vestimentifera and Pogonophora. Journal of the Marine Biological Association of the United Kingdom. 1988;68(3):465–87.
29. Jones ML, Gardiner SL. On the early development of the vestimentiferan tube worm Ridgeia sp. and observations on the nervous system and trophosome of Ridgeia sp. and Riftia pachyptila. The Biological Bulletin. 1989;177(2):254–76.
30. Gardiner SL, Jones ML. On the significance of larval and juvenile morphology for suggesting phylogenetic relationships of the Vestimentifera. American Zoologist. 1994;34(4):513–22.
31. Nussbaumer AD, Fisher CR, Bright M. Horizontal endosymbiont transmission in hydrothermal vent tubeworms. Nature. 2006;441(7091):345–8.
32. Bright M, Eichinger I, von Salvini-Plawen L. The metatrochophore of a deep-sea hydrothermal vent vestimentiferan (Polychaeta: Siboglinidae). Organisms Diversity & Evolution [Internet]. 2013;13(2):163–88. Available from: https://doi.org/10.1007/s13127-012-0117-z
33. Worsaae K, Rouse GW. The simplicity of males: dwarf males of four species of Osedax (Siboglinidae; Annelida) investigated by confocal laser scanning microscopy. Journal of Morphology. 2010;271(2):127–42.

34. Nørrevang A. On the embryology of Siboglinum and its implications for the systematic position of the Pogonophora. Sarsia. 1970;42(1):7–16.
35. Ivanov AV. Analysis of the embryonic development of Pogonophora in connection with the problems of phylogenetics. Journal of Zoological Systematics and Evolutionary Research. 1988;26(3):161–85.
36. Southward EC. A study of the structure of the opisthosoma of Siboglinum fiordicum. The phylogeny and systematic position of Pogonophora. 1975;64–76.
37. Callsen-Cencic P, Flügel HJ. Larval development and the formation of the gut of Siboglinum poseidoni Flügel & Langhof (Pogonophora, Perviata). Evidence of protostomian affinity. Sarsia. 1995;80(2):73–89.
38. Helm C, Weigert A, Mayer G, Bleidorn C. Myoanatomy of Myzostoma cirriferum (Annelida, Myzostomida): Implications for the evolution of the Myzostomid body plan. Journal of Morphology. 2013 Apr;274(4):456–66.
39. Hill SD, Boyer BC. Phalloidin labeling of developing muscle in embryos of the polychaete Capitella sp. I. The Biological Bulletin. 2001;201(2):257–8.
40. Brinkmann N, Wanninger A. Integrative analysis of polychaete ontogeny: cell proliferation patterns and myogenesis in trochophore larvae of Sabellaria alveolata. Evolution & development. 2010;12(1):5–15.
41. Fischer AHL, Henrich T, Arendt D. The normal development of Platynereis dumerilii (Nereididae, Annelida). Frontiers in zoology. 2010;7(1):1–39.
42. Zattara EE, Weisblat D. Cellular and Molecular Mechanisms of Segmentation in Annelida: An Open Question. 2020.
43. Southward EC. Microscopic Anatomy of Invertebrates. Microscopic Anatomy of Invertebrates. 1993;12:327–69.
44. Ivanov AV. Pogonophora. Fauna S.S.S.R. N.S. Vol. 75. Moscow: Academiia Nauk S.S.S.R; 1960. 1–271.
45. Southward EC, Schulze A, Gardiner SL. Pogonophora (Annelida): form and function. Hydrobiologia. 2005;535(1):227–51.
46. Irvine SQ, Chaga O, Martindale MQ. Larval Ontogenetic Stages of Chaetopterus: Developmental Heterochrony in the Evolution of [Internet]. Vol. 197, Bulletin. 1999. Available from: http://www.jstor.orgURL:http://www.jstor.org/stable/1542786
47. Starunov V v, Dray N, Belikova E v, Kerner P, Vervoort M, Balavoine G. A metameric origin for the annelid pygidium? BMC evolutionary biology. 2015;15(1):1–17.
48. Fischer AHL, Henrich T, Arendt D. The normal development of Platynereis dumerilii (Nereididae, Annelida). Frontiers in zoology. 2010;7(1):1–39.
49. Okada K. Annelida. In: Kume M, Dan K, Dan JC, editors. Invertebrate embryology. Nolit; 1968.
50. Tzetlin AB, Filippova A v. Muscular system in polychaetes (Annelida). Hydrobiologia. 2005;535(1):113–26.

51. Bakke T. Settling of the larvae of siboglinum fiordicum webb (Pogonophora) in the laboratory. Sarsia. 1974 Jul 8;56(1):57–70.
52. Rieger RM. A new group of interstitial worms, Lobatocerebridae nov. fam.(Annelida) and its significance for metazoan phylogeny. Zoomorphologie. 1980;95(1):41–84.
53. Filippova A, Purschke G, Tzetlin AB, Müller MCM. Musculature in polychaetes: comparison of Myrianida prolifera (Syllidae) and Sphaerodoropsis sp.(Sphaerodoridae). Invertebrate Biology. 2010;129(2):184–98.
54. Kerbl A, Bekkouche N, Sterrer W, Worsaae K. Detailed reconstruction of the nervous and muscular system of Lobatocerebridae with an evaluation of its annelid affinity. BMC Evolutionary Biology. 2015;15(1):1–34.
55. Southward EC. Development of perviata and vestimentifera (pogonophora). Hydrobiologia. 1999; 402:185–202.
56. Worsaae K, Rimskaya-Korsakova NN, Rouse GW. Neural reconstruction of bone-eating Osedax spp. (Annelida) and evolution of the siboglinid nervous system. BMC evolutionary biology. 2016;16(1):1–23.
57. Iwanoff PP. Die Entwicklung der larvalsegmente bei den Anneliden. Zeitschrift für Morphologie und Ökologie der Tiere. 1928;10(1):62–161.
58. Anderson DT. Embryology and phylogeny in Annelids and Arthropods. Oxford: Pergamon Press. 495 p. 1973.
59. Fischer AHL, Arendt D. Mesoteloblast-like mesodermal stem cells in the polychaete annelid Platynereis dumerilii (Nereididae). Journal of Experimental Zoology Part B: Molecular and Developmental Evolution. 2013;320(2):94–104.
60. Seaver EC, Thamm K, Hill SD. Growth patterns during segmentation in the two polychaete annelids, Capitella sp. I and Hydroides elegans: comparisons at distinct life history stages. Evolution & development. 2005;7(4):312–26.
61. Jägersten G. Beobachtungen über Myzostomum cirriferum. Arkiv Zool. 1940; 32:1–6.
62. Kristof A, Wollesen T, Maiorova AS, Wanninger A. Cellular and muscular growth patterns during sipunculan development. Journal of Experimental Zoology Part B: Molecular and Developmental Evolution. 2011;316(3):227–40.

Figures

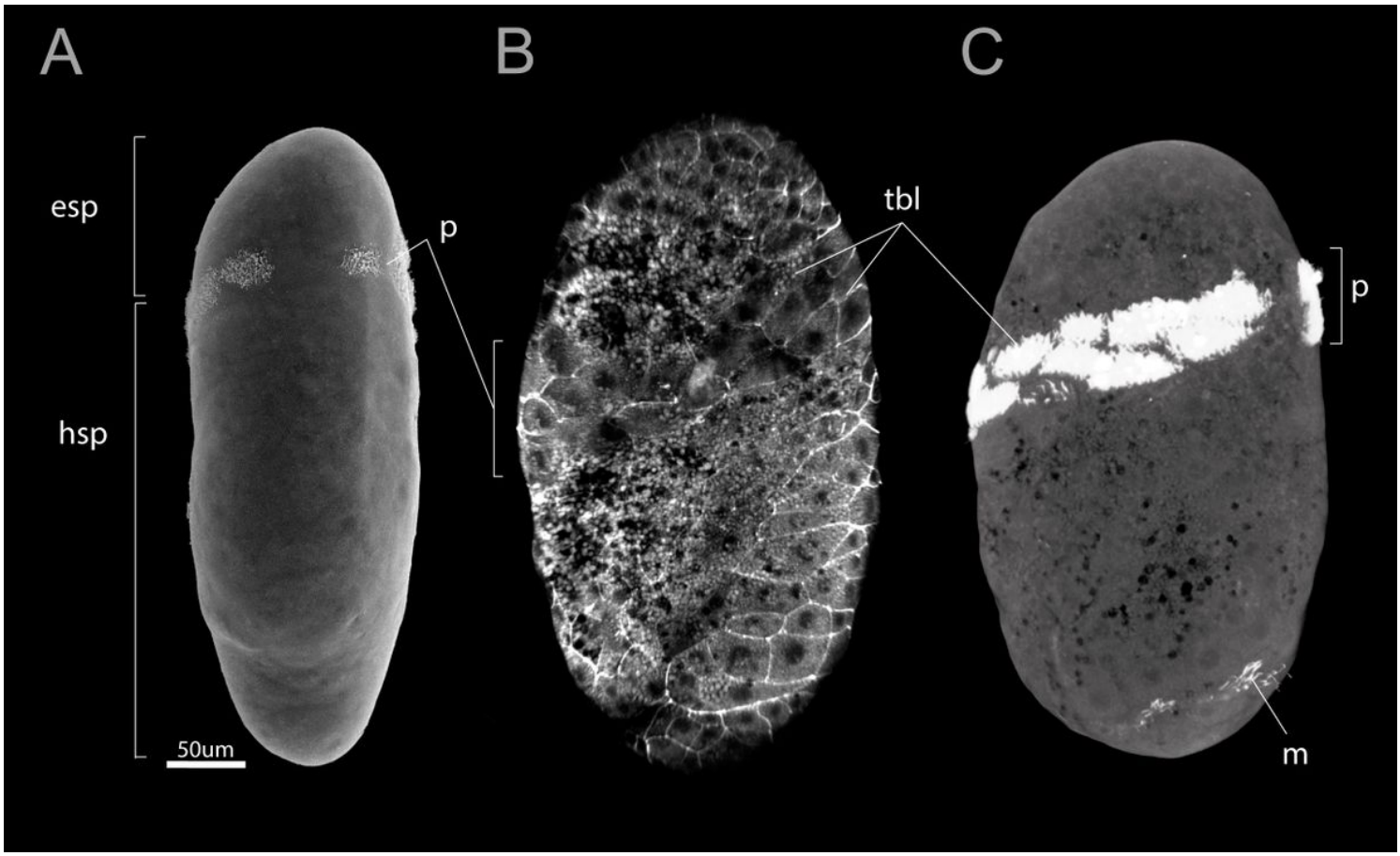

Figure 1

Trochophores of Siboglinum fiordicum. A – an early trochophore with prototroch (SEM). B, C – late trochophore with the prototroch and irregular mesotroch, CLSM of the staining with phalloidin (B) and anti-α-tubulin (C). esp – episphere, hsp – hyposphere, m – mesotroch, p – prototroch, tbl – trochoblasts.

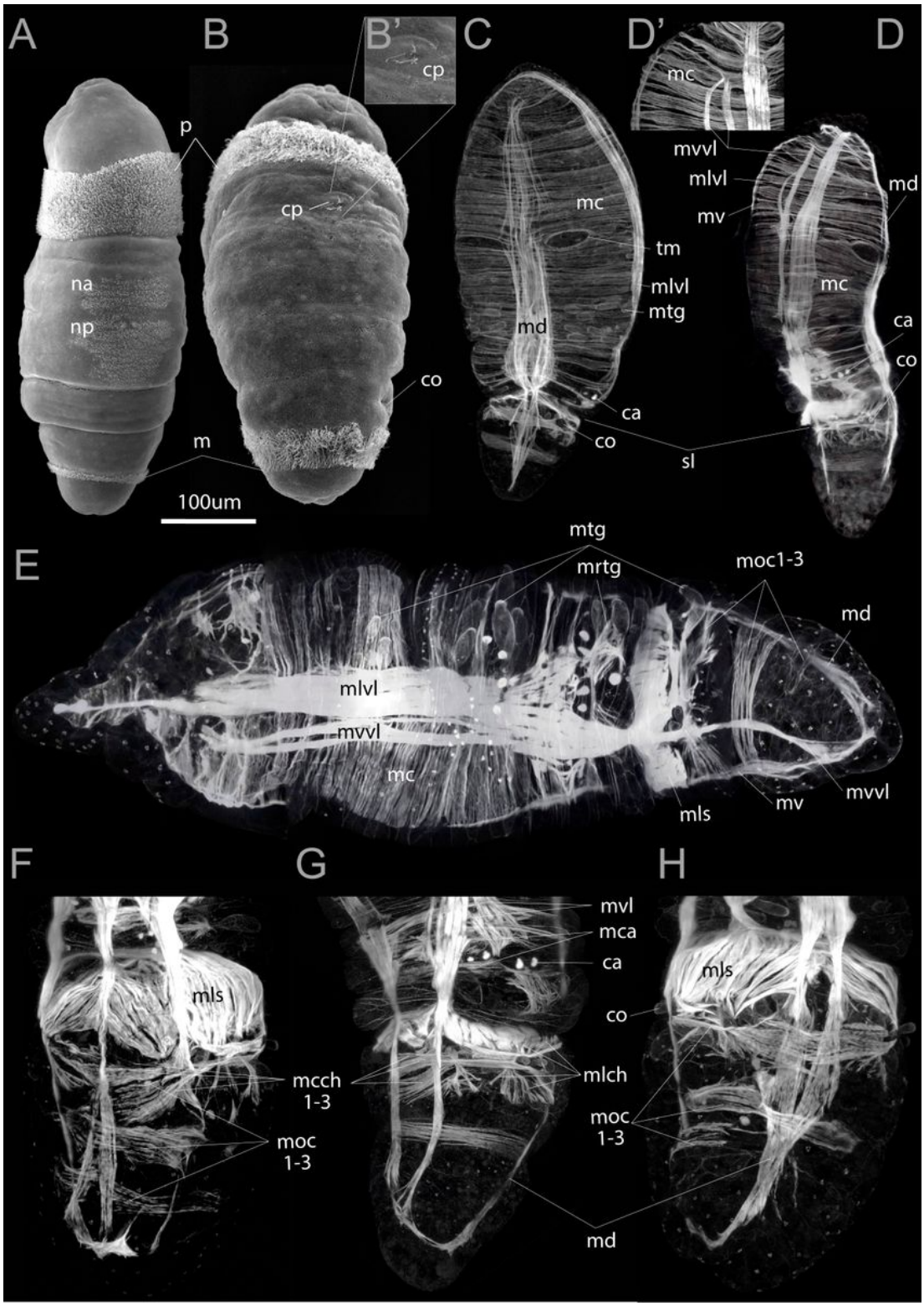

Figure 2

Early metatrochophora of Siboglinum fiordicum, by SEM (A, B) and phalloidin staining and CLSM (C-H). A, B – ventral and dorsal view of the larva in that the first septum internally divides body into two tagmas: common anterior segment and common opisthosomal segment. Dorsal side distinguished by the presence of the ciliary spot (cp) (b). C – dorsal view of the larva, distinguished by the presence of the single dorsal longitudinal muscle strand (md) and asymmetric tentacular muscles (tm). D, E – left lateral

view distinguished by the presence of the ventrolateral longitudinal muscle strands (mvvl, mlvl) and layer of circular muscles in the anterior part of the body. Circular muscles encircle the body and overlap on the ventral (d) and dorsal sides of the body. F-H – ventral, lateral, dorsal views of the opisthosoma bearing three first circular bands (moc1-3). ca – annular chaetae, co – opisthosomal chaetae, cp – dorsal ciliary spot, m – mesotroch, mc – circular musculature, mca – muscles of annular chaetae, mcch1-3 – circular muscles of the chaetal apparatus, md – dorsal longitudinal muscle strand, mlch – longitudinal muscles of the chaetal apparatus, mls – longitudinal muscle of the first septum, mlvl – lateral component of the ventrolateral longitudinal muscle strand, moc1-3 - circular muscles in the opisthosoma, mrtg – radial muscles interconnecting mtg and longitudinal muscle strands, mtg - muscles of the tubiparous glands, mv – ventral longitudinal muscle strand, mvvl – ventral component of the ventrolateral longitudinal muscle strand, na – anterior neurotroch, np - posterior neurotroch, p – prototroch, sI – place of the firsth septum, tm – muscle bundles of the tentacular anlage.

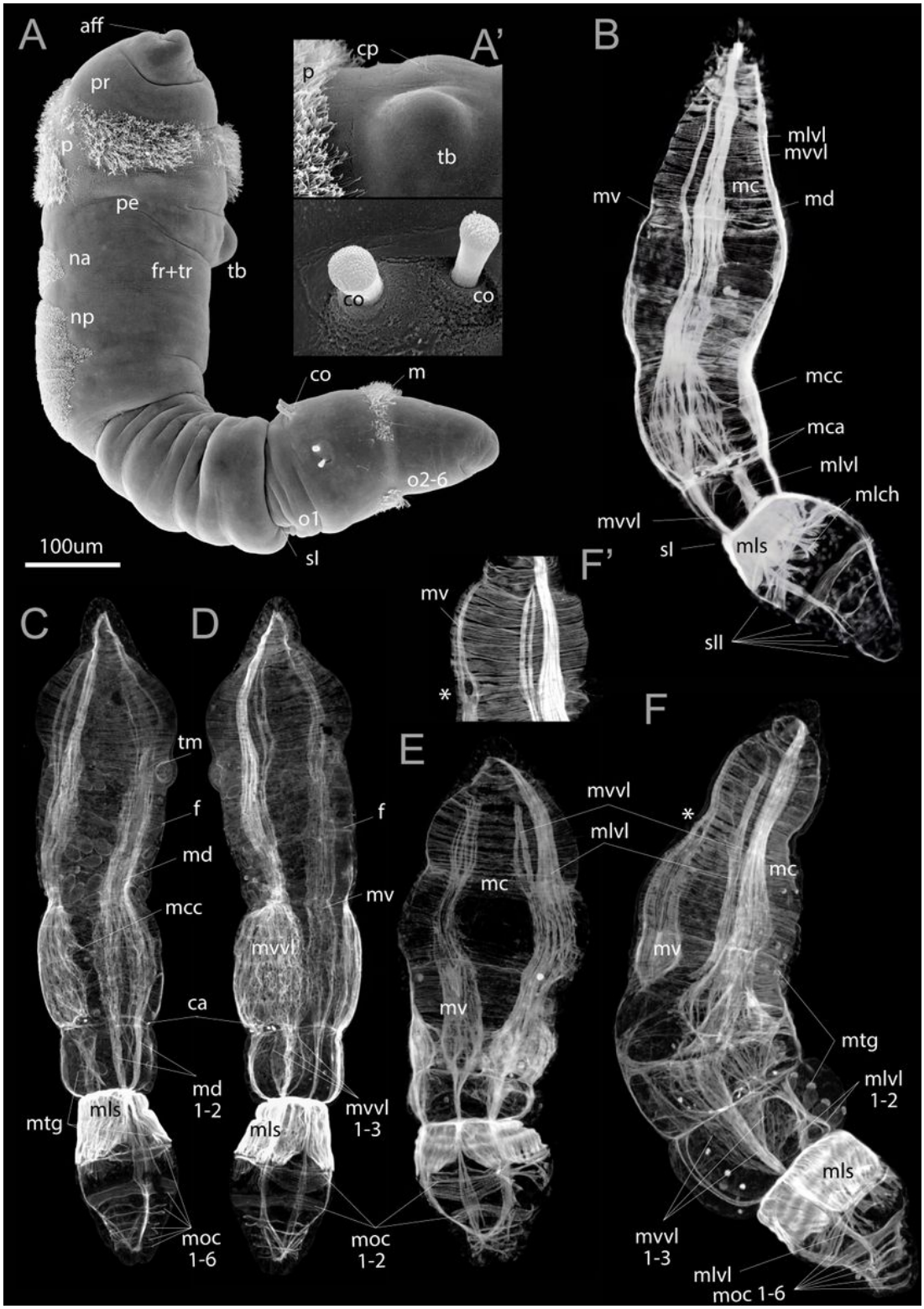

Figure 3

Early metatrochophora of Siboglinum fiordicum, by SEM (A) and phalloidin staining and CLSM (B-F). A – lateral view of the larva with the visible first septum dividing common anterior segment (fr+tr) from the segmented opisthosoma (o1, o2-6), it has opisthosomal chaetae (co) and bud of future tentacle (tb) which are also shown in (a). B, C, D – lateral, dorsal and ventral views of the metatrochophores with well-developed longitudinal and circular musculature. At this stage, the muscles of the first septa remarkably

increase, six circular bands marking position of the opisthosomal septa are formed, the musculature of the first opisthosomal chaetae is formed. E-F – ventral and lateral view of the larvae showing the muscles contraction during the larval movement. Metatrochophores have the holes in the ventral strand in (f) which is the atavism of the mouth which was opened and functional in the ancestors (shown by *). aff – frontal fold, ca – annular chaetae, co – opisthosomal chaetae, cp – dorsal ciliary spot, f – frenulum, fr+tr – common anterior segment, m – mesotroch, mc – circular musculature, mca – muscles of annular chaetae, mcc – lateral circular muscle fibers interconnecting the longitudinal strands, md – dorsal longitudinal muscle strand, md1-2 – two components of md in the postannular trunk segment, mlch – longitudinal muscles of the chaetal apparatus, mls – longitudinal muscle of the first septum, mlvl – lateral component of the ventrolateral longitudinal muscle strand, mlvl1-2 – two components of mlvl in the postannular trunk segment, moc1-6 - circular muscles in the opisthosoma, mtg - muscles of the tubiparous glands, mv – ventral longitudinal muscle strand, mvvl – ventral component of the ventrolateral longitudinal muscle strand, mvvl1-3 - three components of mvvl in the postannular trunk segment, na – anterior neurotroch, np - posterior neurotroch, p – prototroch, pe – peristomium, pr – prostomium, sI – the first septum in the larval ontogenesis, sII – the second septum in order of formation, tb – tentacular anlage, tm – muscle bundles of the tb.

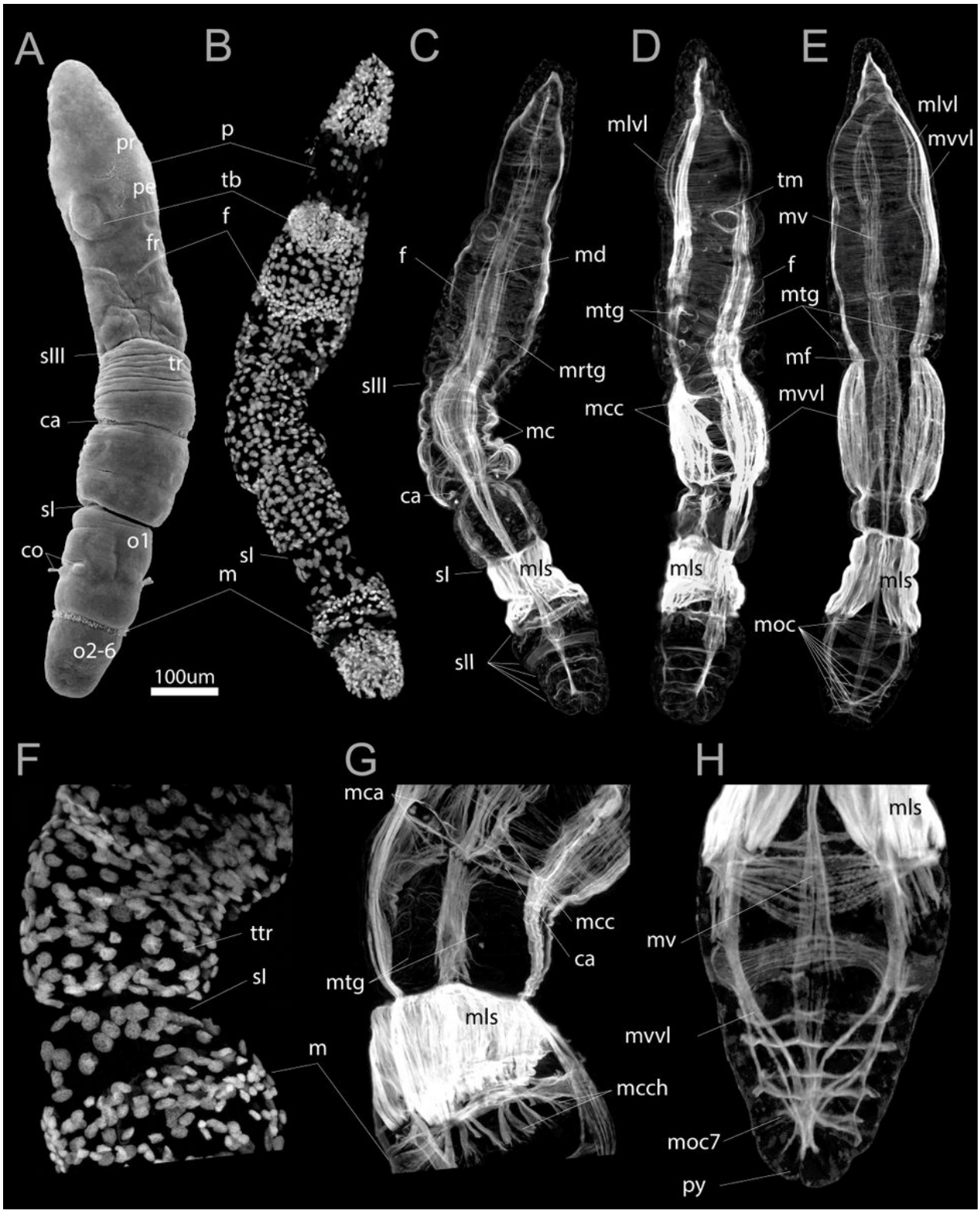

Figure 4

Competent larva of Siboglinum fiordicum, by SEM (A) and phalloidin and DAPI staining visualized by CLSM (B-H). A – dorsal view of the competent larva having the prostomium (pr), peristomium (pe), forepart segment (fr), trunk segment (tr), ca 6 opisthosomal segments (o1, o2-6). C – DAPI staining marks the accumulation of cells in the region of the tentacle rudiment (tb), frenulum (f), and vice versa, the rare location of large cells, such as trochoblasts of the prototroch (p) and mesotroch (m), and

myoepithelial cells that form the muscles of the first septum (sI). C, D, E – dorsal, lateral and ventral views of the competent larvae with the circular musculature in the anterior end and almost complete layers of the prominent longitudinal musculature in the posterior end of larva. Note in (C, D) the periglandular musculature (mtg) which are equipped with the radial fibers extending from the main longitudinal strand (mrtg). F, G – DAPI and phalloidin stainings the postannular area of the trunk segment (ttr), which will encompass the trophosome in juveniles. H – ventral view of the opistosoma, the seventh circular muscle added (moc7) at the posteriormost end, pygidium is hardly distinguished (py). ca – annular chaetae, co – opisthosomal chaetae, f – frenulum, fr – forepart, m – mesotroch, mc – circular musculature, mca – muscles of annular chaetae, mcc – lateral circular muscle fibers interconnecting the longitudinal strands, mcch - circular muscles of the chaetal apparatus, md – dorsal longitudinal muscle strand, mf – anterior circular muscle of the sIII, mls – longitudinal muscle of the first septum, mlvl – lateral component of the ventrolateral longitudinal muscle strand, moc – circular muscles in the opisthosoma, mrtg – radial muscles interconnecting mtg and longitudinal muscle strands, mtg - muscles of the tubiparous glands, mv – ventral longitudinal muscle strand, mvvl – ventral component of the ventrolateral longitudinal muscle strand, o1-o2 - the first-sixth segments of the opisthosoma, p – prototroch, pe – peristomium, pr – prostomium, py – pygidium, sI – the first septum in the larval ontogenesis, sII – the second septum in order of formation, sIII – the third septum in order of formation, tb – tentacular anlage, tm – muscle bundles of the tb, tr – trunk segment.

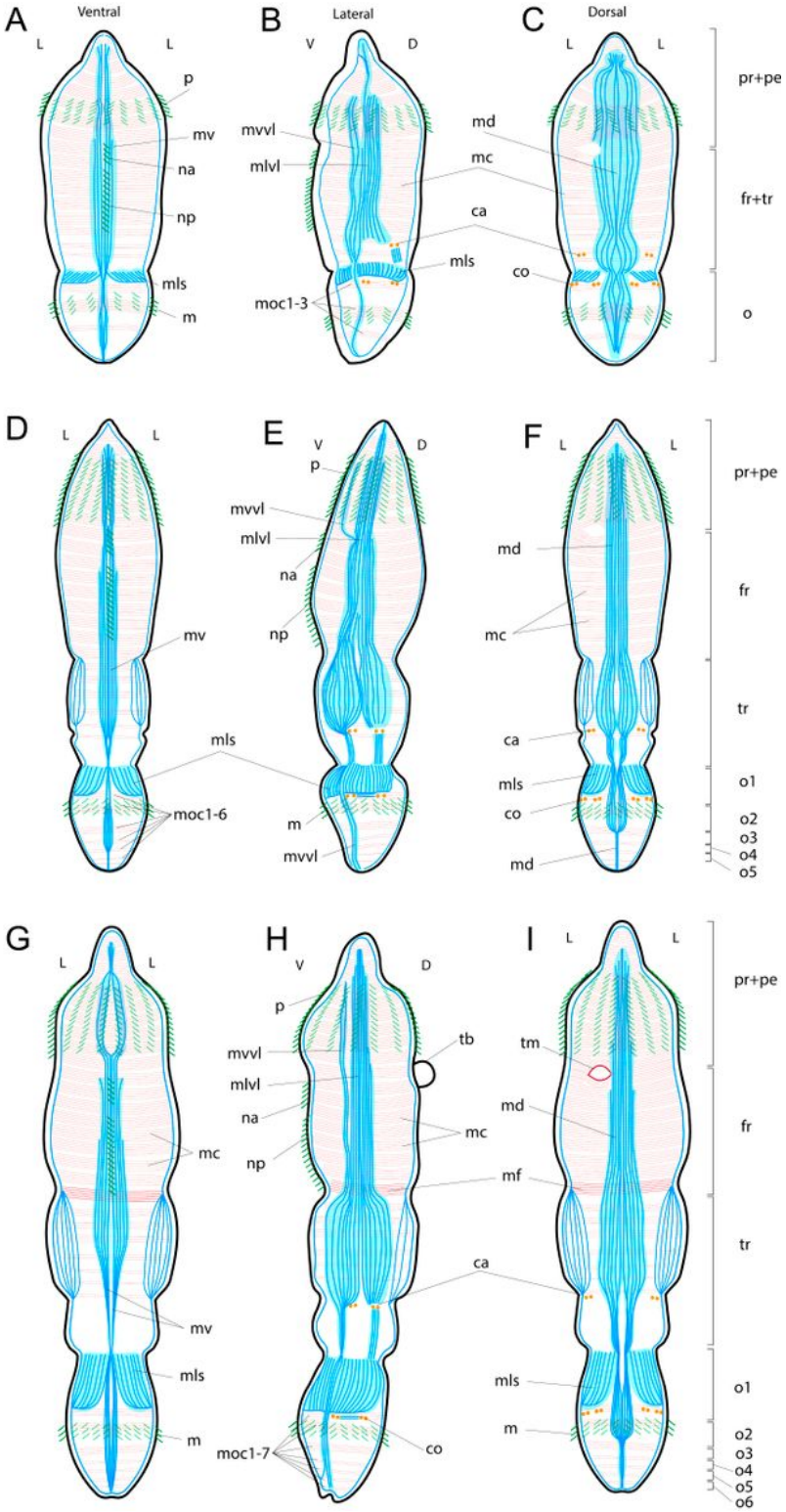

Figure 5

Schematic drawings of the myognesis in Siboglinum fiordicum larvae. A-C – early metatrochophora, the first septum divides body into two tagmas: common anterior segment (fr+tr) and common opisthosomal segment (o), D-F - late metatrochophora, division of the opisthosoma into segments, G-I – competent larva, division of the common anterior segment into forepart (fr) and trunk (tr) and new posterior segments appear at the end of the opisthosoma. Longitudinal muscles are shown in blue, circular

muscles are in red, cilia - in green, chaetae - in orange. L, V, D serve for lateral, ventral and dorsal body orientations. ca – annular chaetae, co – opisthosomal chaetae, fr - forepart segment, m – mesotroch, mc – circular musculature, md – dorsal longitudinal muscle strand, mls – longitudinal muscle of the first septum, mlvl – lateral component of the ventrolateral longitudinal muscle strand, moc1-7 – the first-seventh circular muscles in the opisthosoma, mv – ventral longitudinal muscle strand, mvvl – ventral component of the ventrolateral longitudinal muscle strand, na – anterior neurotroch, np – posterior neurotroch, o – common segment of the opisthosoma, o1-o6 – the first-sixth segments of the opisthosoma, p – prototroch, pe – peristomium, pr – prostomium, tb – tentacular anlage, tm – circular muscles of the tb, tr - trunk segment.

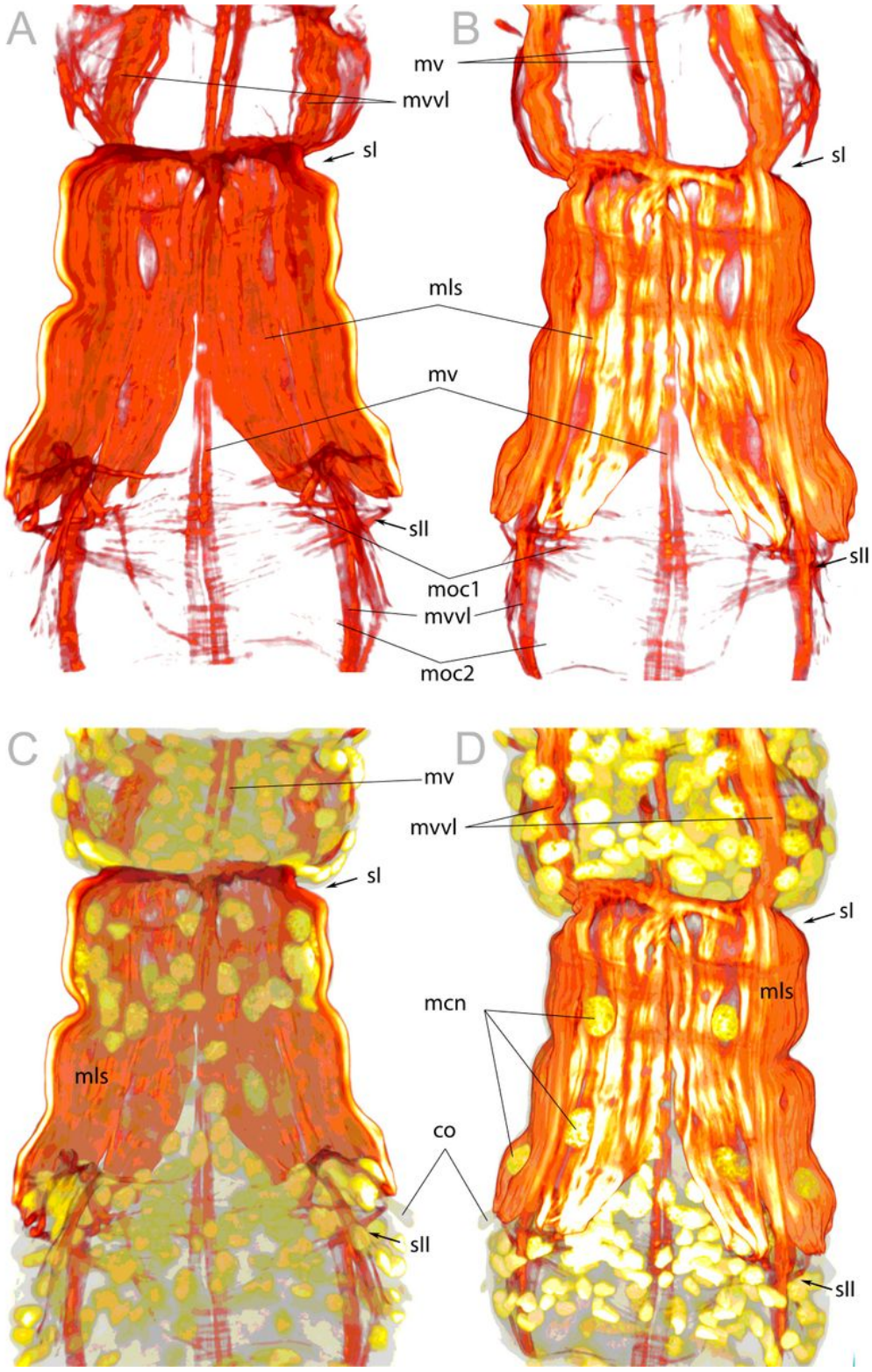

Figure 6

Musculature of the first septum in the late metatrochophora of Siboglinum fiordicum. Surface rendering in AMIRA of the longitudinal muscles of the first septum between trunk segment and the first segment of the opisthosoma. Musculature is shown in red; nuclei stained with DAPI as well as autofluoresce of the opisthosomal chaetae are shown in yellow. A, C – ventral view from the inside the body of the larva. B, D – ventral view from the outside the larva. co – opisthosomal chaetae, mcn – nuclei of large myoepithelial

cells of the 1st septum, mls – longitudinal muscles of the first septum, moc1-2 – the first and the second circular muscle bundles in opisthosoma, mv – ventral longitudinal strand, mvvl – ventral component of the ventrolateral longitudinal muscle strand, sI – the first septum in the larval ontogenesis, sII – the second septum in order of formation.

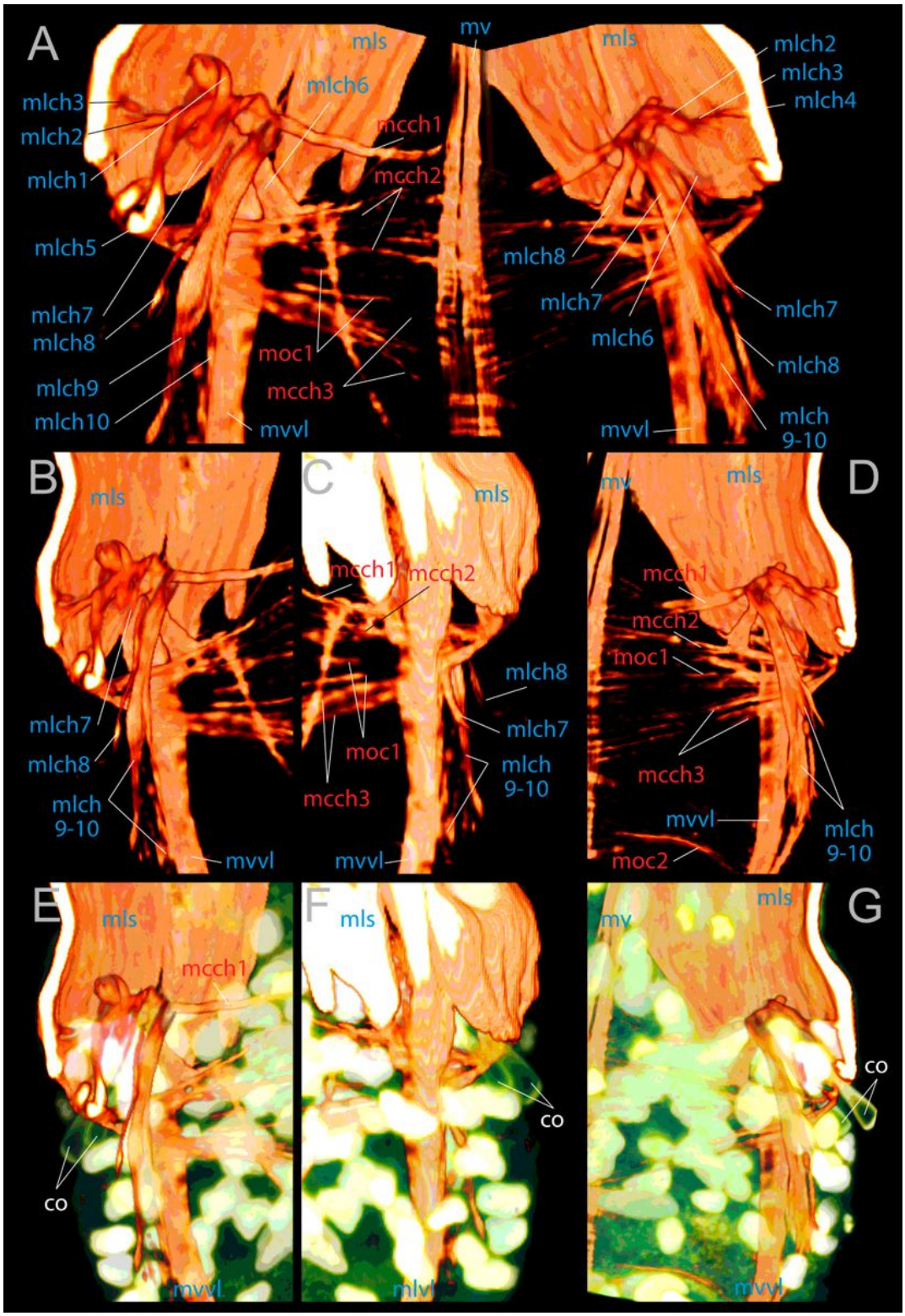

Figure 7

Muscles of the opisthosomal chaetae in the competent larva of Siboglinum fiordicum. Surface rendering in AMIRA of the longitudinal muscles of the first septum between trunk segment and the first segment of the opisthosoma. Musculature is shown in red; nuclei stained with DAPI as well as autofluoresce of the opisthosomal chaetae are shown in yellow. A - ventral view from the inside the larva body; B, E – ventral view of the left side from the inside the larva body; C, F – the same fragment from the outside; D, G - ventral view of the right side from the inside. co – opisthosomal chaetae; mcch1-3 – circular muscles of the chaetal apparatus, mlch1-10 – longitudinal muscles of the chaetal apparatus, mls - longitudinal muscles of the first septum, mvvl – ventral component of the ventrolateral longitudinal muscle strand, moc1-2 - the first and the second circular muscle bundles in the opisthosoma, mv – ventral longitudinal strand.

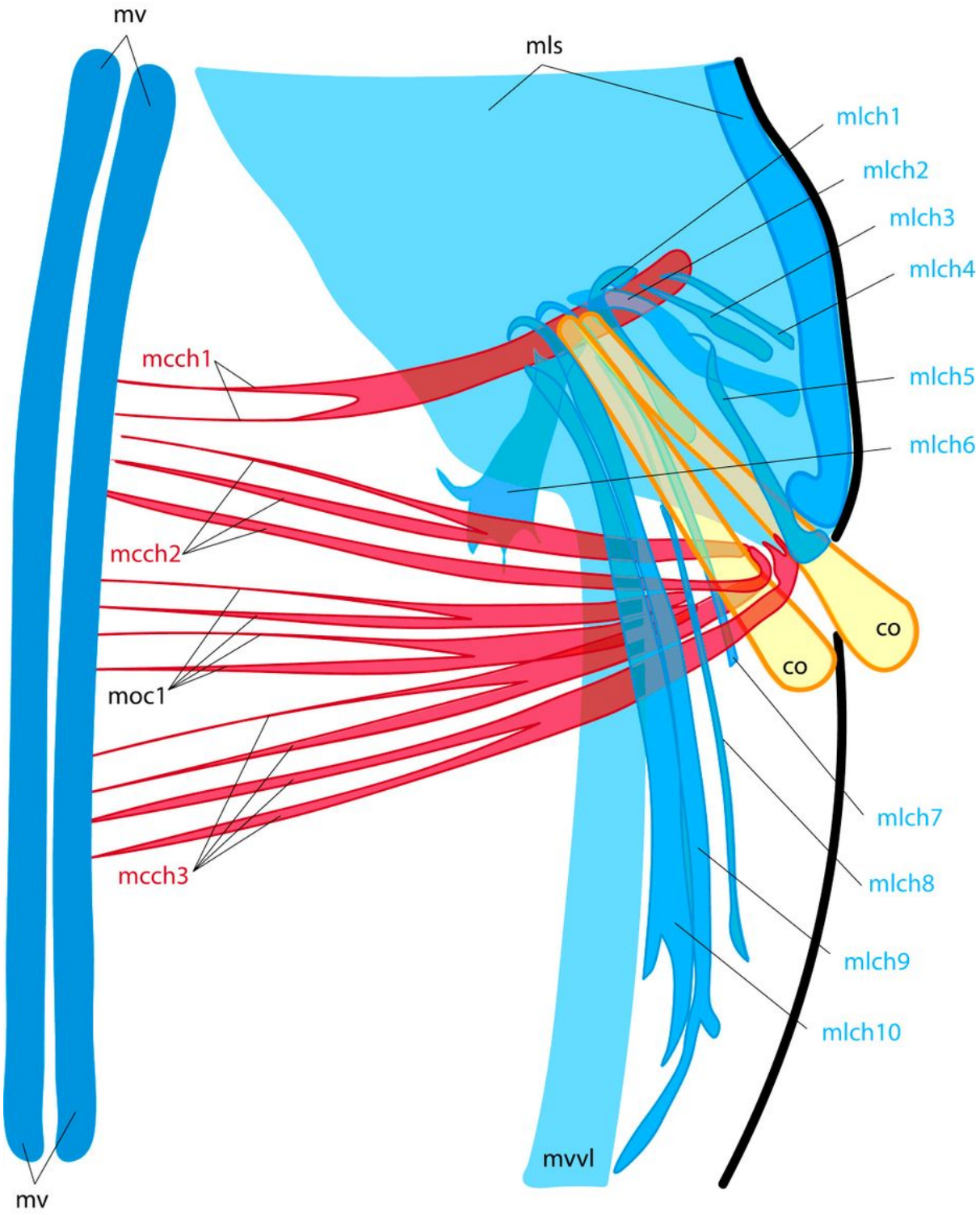

Figure 8

Schematic drawings of muscles of the opisthosomal chaetae in the competent larva of Siboglinum fiordicum. The scheme is based on the CLSM data. The ventral view of the level of the opisthosomal chaetae from the inside of the larva. Longitudinal muscles are shown in blue, circular muscles are in red, chaetae - in yellow. co – opisthosomal chaetae; mcch1-3 – circular muscles of the chaetal apparatus, mlch1-10 – longitudinal muscles of the chaetal apparatus, mls - longitudinal muscles of the first septum,

mvvl – ventral component of the ventrolateral longitudinal muscle strand, moc1 - the first circular muscle bundles in the opisthosoma, mv – ventral longitudinal strand.

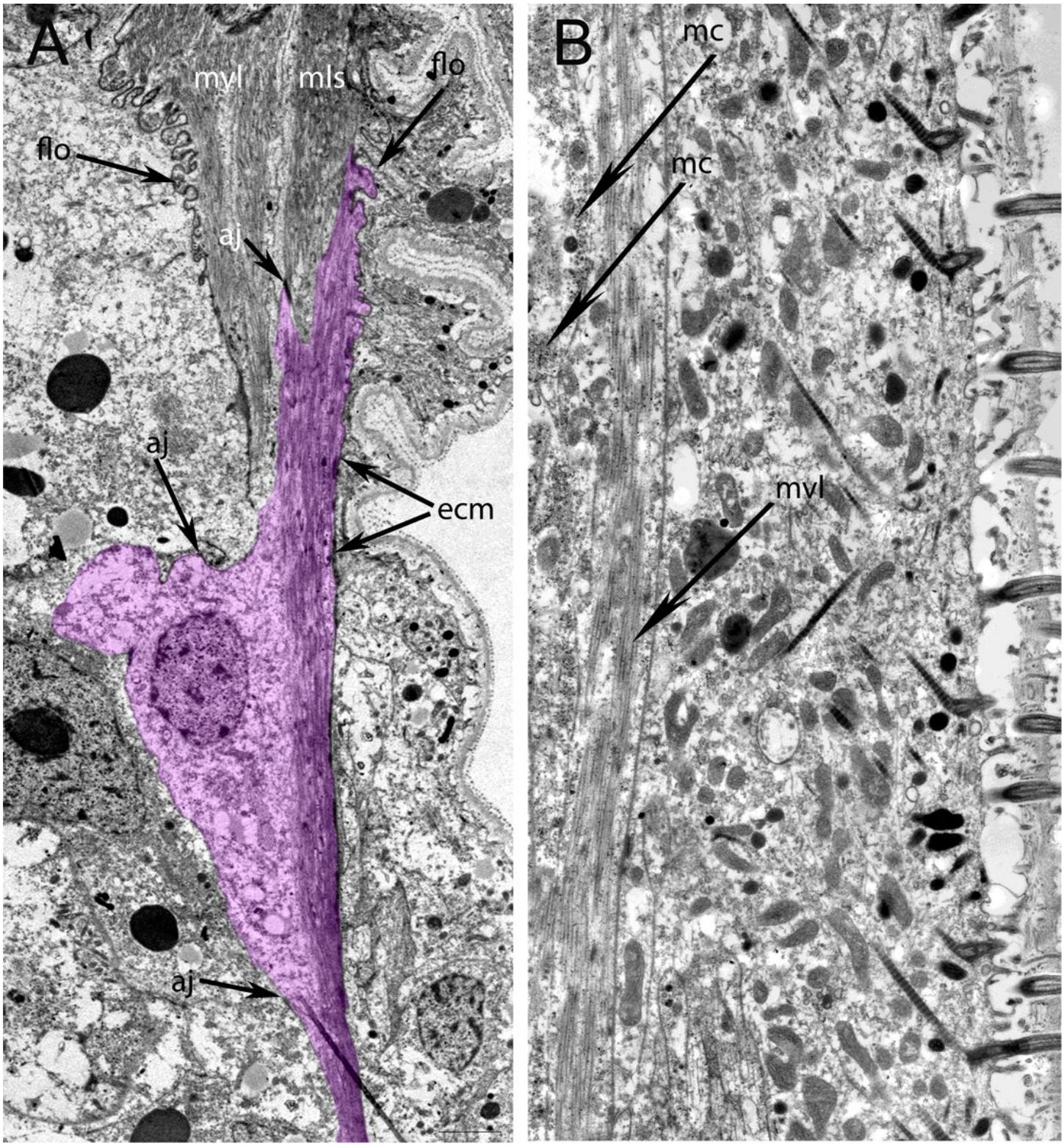

Figure 9

Ultrastructure of somatic musculature, the parafrontal sections of metatrochophora of Siboglinum fiordicum. A – left ventrolateral longitudinal muscle (mvl) strand extending from the trunk segment to the first segment of opisthosoma, and septal longitudinal muscle (mls) bands extending from the septum I to

the opisthosome. Coelom of opisthosoma lined with the large myoepithelial cells (marked in purple). B – circular muscles (mc) lie inner to the longitudinal muscles, at the prototroch level. aj – adherens junction, ecm – extracellular matrix, flo – finger-like outgrowths, mc – circular muscles, mls – longitudinal muscles of the first septum, mvl – ventrolateral longitudinal muscle strand.

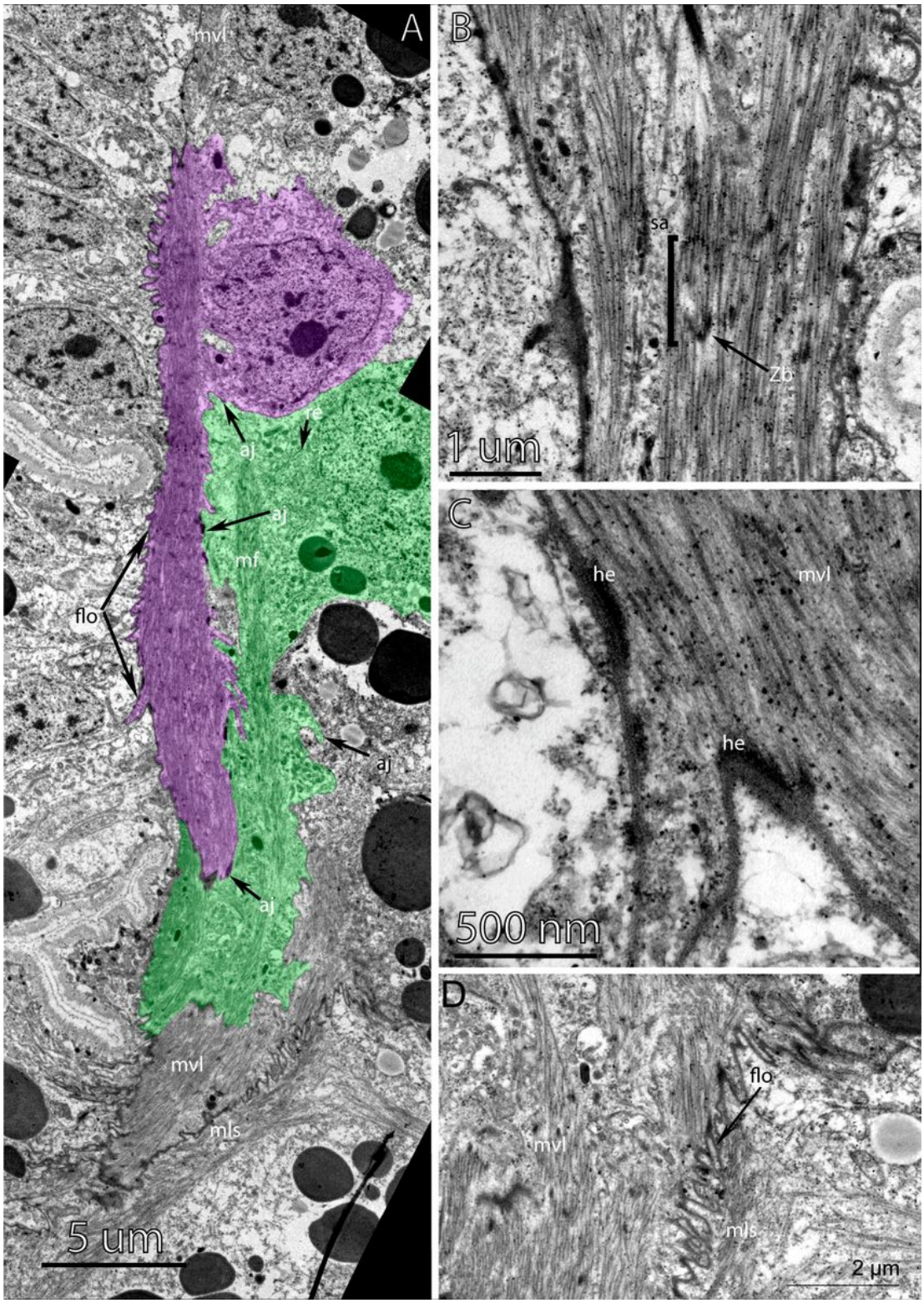

Figure 10

Ultrastructure of the ventrolateral longitudinal muscle (mvl), parafrontal sections of the metatrochophora of Siboglinum fiordicum. A – the myoepithelial cells of the somatic longitudinal musculature form pseudo-multilayer (cells shown in different colors). Highly folded ECM along the contracted right ventrolateral longitudinal muscle (mvl). B – ultrastructure of the sarcomere of the striated muscles. C – hemidesmosomes (he) of the muscle fibers. D – site of the highly folded ECM (flo) of the septum and basal membrane of the myoepithelial cell: mvl from the trunk attaches to the ecm of the septum I. aj – adherens junction flo – finger-like outgrowths, he – hemidesmosomes, mf – longitudinal myofilaments, mls - longitudinal muscles of the first septum, mvl – ventrolateral longitudinal muscle strand, re – rough endoplasmic reticulum, sa – sarcomere, Zb – Z-bodies.

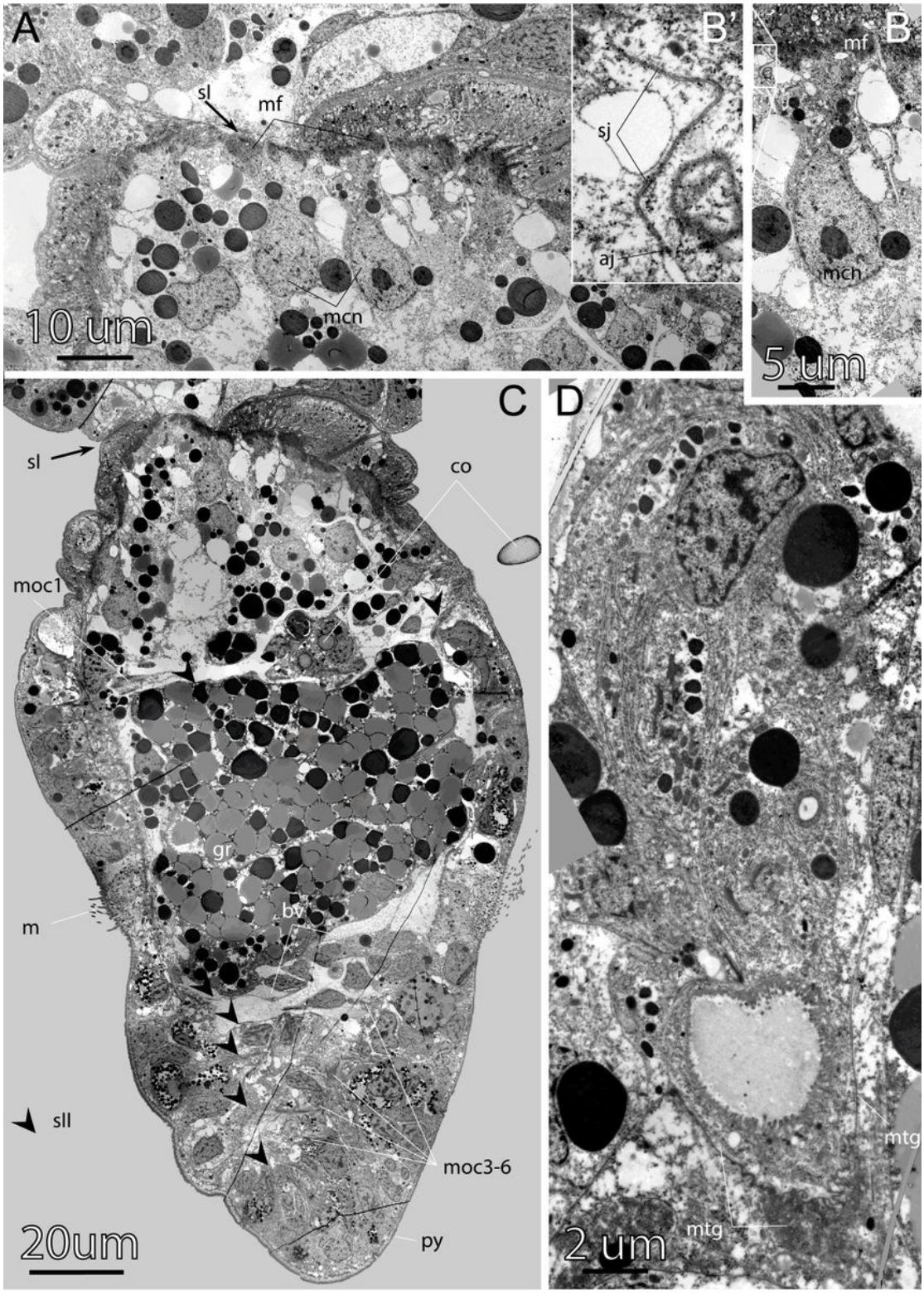

Figure 11

Ultrastructure of the first septum and opisthosomal segments of the late metatrochophora of Siboglinum fiordicum, parasagittal sections. A – the first septum formed by bottleneck-shaped myoepithelial cells. B - myoepithelial cell of the first septum bearing the myofilaments. b - cells contacted with adherens junctions (aj) and septate junction (sj). C – the sagittal section of the segmented opisthosoma, segments are divided by non-muscular septa, which are the second in order of formation (sII), marked by

arrowheads. sII at this stage is just thin layers of the ECM (sometimes with blood), they have no muscle fibers, but they contacted to the myoepithelial cells of the body wall (at place of moc1-6). D – tubiparous glands secreting the tube material, note the cup-shapes microvilli facing he lumen of the gland. Thin layer of the muscle surrounding the gland, especially around the developing glandular duct, which supposedly pushes the tube secrete outside when muscles contracted. aj - adherens junctions, bv – blood vessel, co - opisthosomal chaetae, gr – gut rudiment, m – mesotroch, mcn – large nuclei of the longitudinal myoepithelial cells, mf – myofilaments, moc1-6 – the first-sixth circular muscle bundles in the opisthosoma, mtg – musculature of the tubiparous gland, py – pygidial area, sj - septate junction, sI – the septum that is formed the first in order of formation, dividing trunk and the first opisthosomal segments, sII - the septa that are formed second in order of formation, dividing the opisthosomal segments, simultaneously formed.

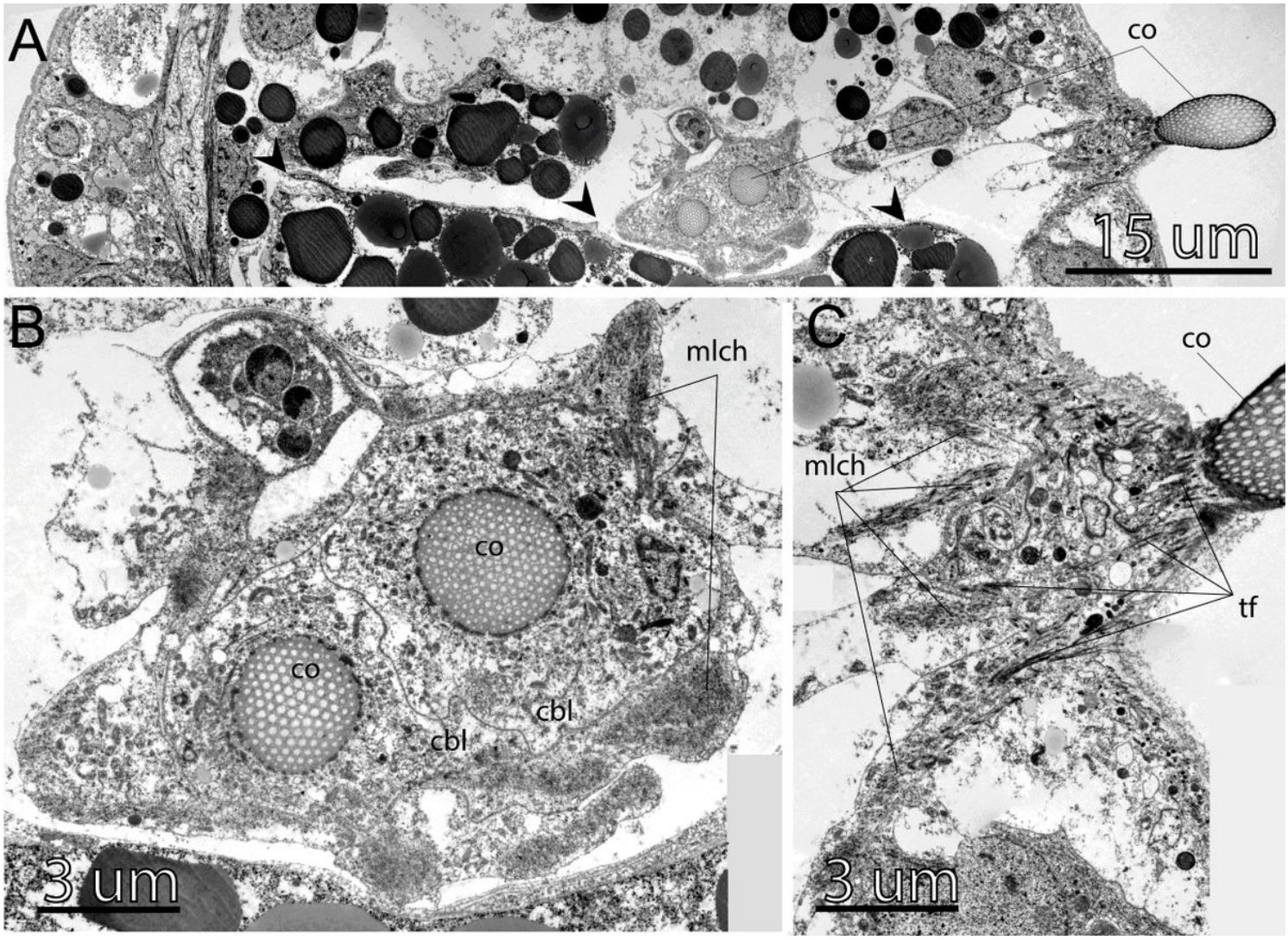

Figure 12

Ultrastructure of chaetal muscles of late metatrochophora of Siboglinum fiordicum. A-C – ultrastructure of the muscle fibers of the chaetal sacs at the parasagittal sections. A – overview of the chaetae position in the first opisthosomal segment; arrowheads show the non-muscular second septum. B – close-up of the chaetal sac formed by the longitudinal muscle bundles and chaetoblasts, C – the chaetae raised by

muscles, the muscles are attached to the cuticle through tonofilaments. cbl - chaetoblast, co – opisthosomal chaetae, mlch - longitudinal muscles of the chaetal apparatus, tf – tonofilament.

Supplementary Files

This is a list of supplementary files associated with this preprint. Click to download.

- Additfile1Moviesiboglinum.mp4